FACIES ARCHITECTURE OF AN ARID DEPOSITIONAL SYSTEM WITHIN THE EL RENO GROUP (PERMIAN) OF WESTERN OKLAHOMA

By

TYLER M. TREECE

Bachelor of Science in Geology

Arkansas Tech University

Russellville, AR

2007

Submitted to the Faculty of the
Graduate College of the
Oklahoma State University
in partial fulfillment of
the requirements for
the Degree of
MASTER OF SCIENCE
July, 2009

FACIES ARCHITECTURE OF AN ARID COASTLINE

WITHIN THE PERMIAN ROCKS OF WESTERN

OKLAHOMA

Thesis Approved:

Dr. Alexander R. Simms

Thesis Adviser

Dr. Jay M. Gregg

Dr. Darwin R. Boardman

Dr. A. Gordon Emslie

Dean of the Graduate College

ACKNOWLEDGMENTS

I would first like to thank the U.S. Geological Survey, National Cooperative Geologic Mapping Program, under assistance Award No. 08HQAG0046 for funding this thesis. A special thanks goes to Steve Chipera and Chesapeake Energy for running x-ray diffraction on shale samples. I would also like to say thanks to my advisor, Dr. Alex Simms for providing me the opportunity to work on this project and for all of the guidance along the way. Thank you to Dr. Tom Stanley and Dr. Neil Suneson of the Oklahoma Geological Survey for help with initial formation identification in the field. I would also like to thank all of the faculty at Oklahoma State University for the incredible learning experience that OSU provided me. A special thank you goes to my committee members, Dr. Jay Gregg and Dr. Darwin Boardman, for the helpful suggestion provided during the review process. Gratitude is due to all of the land owners in my study area, that are too numerous to name, for allowing access to complete my field mapping. Thank you to Chesapeake Energy and the Oklahoma Geological Society for providing scholarship funding to me for completion of my thesis. Thank you to all of the friends that I have met at OSU for providing moral support along the way. Thanks to my parents, Scott and Pamm Treece for encouraging me to pursue a master degree. Finally, I would like to thank my fiancée, Lindsey Arnold for all of the loving support she has given me.

TABLE OF CONTENTS

Chapter Page

LIST OF TABLES

LIST OF FIGURES

Figure Page

CHAPTER I

INTRODUCTION

Red Beds of central North America cover approximately four percent of the continent (Tomlinson, 1916; Fig. 1). Though these Red Bed deposits are wide spread, much of the detailed work determining their depositional environments has focused on the western US (Gustavson *et al.*, 1980; Handford and Fredericks, 1980; Handford, 1981; Presley, 1981; Speer, 1983; Presley, 1987; Andreason, 1992; Mack *et al.*, 1995; Lucas *et al.*, 1999; Lucas *et al.*, 2001; Mack, 2007), with little detailed work done in Oklahoma. The Red Beds of Oklahoma are a potential source of copper resources (Heine, 1975; Cox and Al-Shaieb, 1980; Yang, 1985; Fay and Brockie, 2002), provide important water resources (Osborn *et al.*, 1998; Johnson, 2003; Paxton *et al.*, 2004), and the dissolution of gypsum layers during drilling may provide shallow hazards to oil and gas exploration. Previous work on the Duncan Formation of the North American mid-continent has interpreted this formation as fluvial deltaic (Sawyer, 1924; Gould, 1926; Becker, 1930; Green, 1937; Fay, 1964) and little recent detailed work has been conducted on the depositional environments of these units. One problem with early interpretations is that the large fluvial environments that would be needed to deposit the thick sequences of shale and sand do not fit into current climate models for the Permian of central North

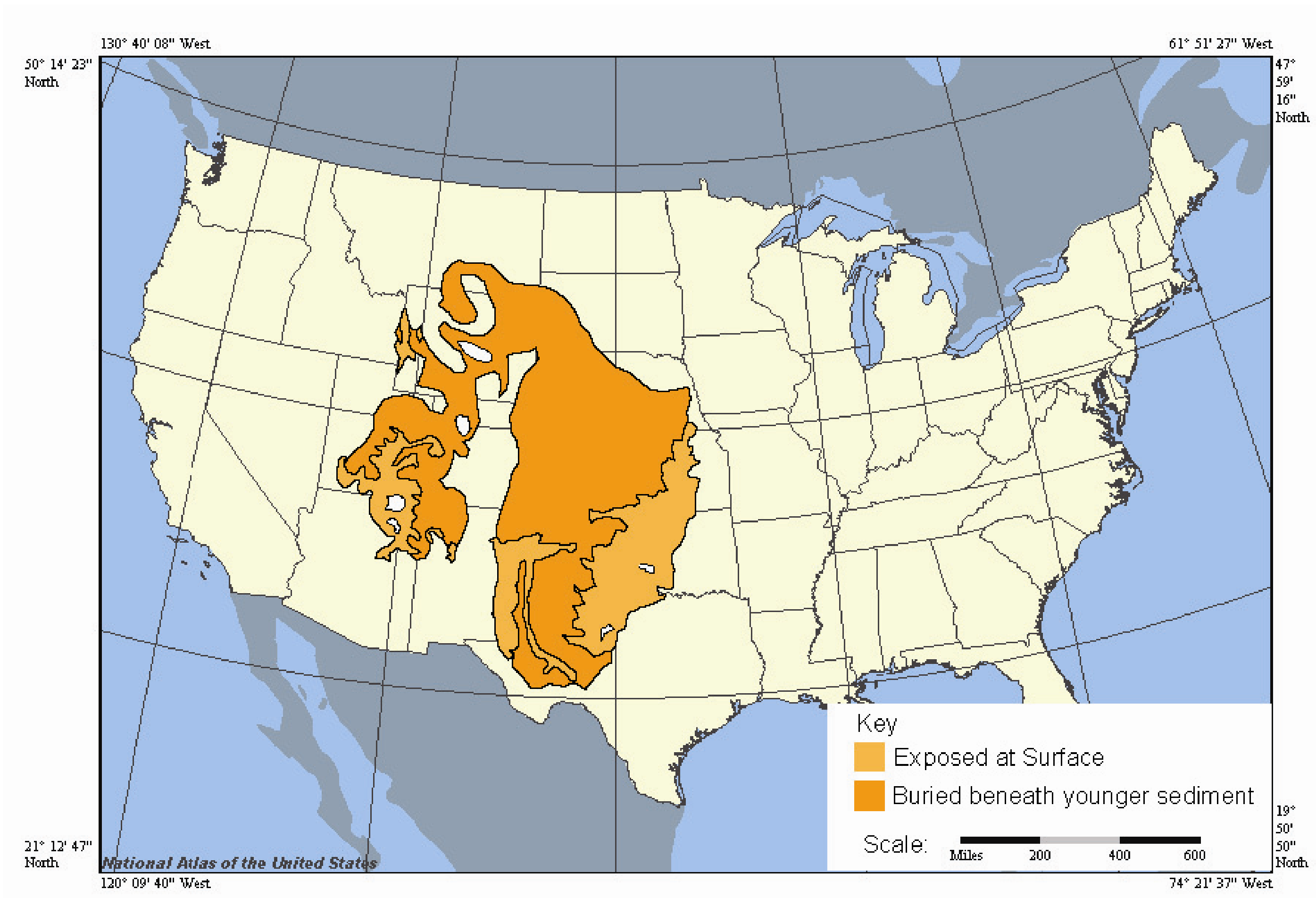

Figure 1-Map showing approximate distribution of North American Red beds. Modified from Tomlinson (1914).

America. These recent climate models for the Permian mid-continent point to a dry climate and suggest eolian processes were an important agent acting on the landscape (Tabor and Montañez, 2004; Tabor and Montanez, 2005; Peyser and Poulsen, 2008; Soreghan *et al.*, 2008a).

Classic facies models of shallow marine systems such as those of deltas (e.g. Galloway, 1975; Bhattacharya and Giosan, 2003) and estuaries (e.g. Dalrymple *et al.*, 1992) may not apply very well to fine grained arid environments . Recent work from the Solway Basin (Permian) in the United Kingdom has outlined the characteristics of deposits formed in arid systems with a large influx of fine-grained material (Brookfield, 2008). Brookfield (2008) compared the hyperarid intracontinental Solway Basin to modern lake deposits in the hyperarid deserts of north central Africa and central Australia where recent work has documented the importance of terminal splays and playa lakes upon the landscape (Tooth, 1999; Lang *et al.*, 2004; Tooth, 2005; Fisher *et al.*, 2008).

The El Reno Group (Permain) of the North American mid-continent provides an excellent place to reevaluate these early depositional models for the Red Beds of Oklahoma. Within the El Reno Group fine grained sandstones, shales, and mudstone conglomerates of the Duncan Formation grade into shales of the Dog Creek and Flowerpot Shales, and the shales, gypsum, and dolomites of the Blaine Formation. The purpose of this project is to reexamine the El Reno Group and determine if the depositional environments are consistent with classic models of shallow marine systems or depositional systems that may have formed within more arid environments. It is hypothesized that the Duncan Formation will not fit more traditional models of deltas or other shallow marine systems as determined by previous authors (Sawyer, 1924; Gould, 1926; Becker, 1930; Green, 1937; Fay, 1964), but represents an arid-land depositional system. Through the use of geological mapping on topographic maps at a 1:24,000 scale, detailed measured sections, examination of thin sections, and x-ray diffractometry (XRD) of shale samples, a facies model was developed for the Duncan Formation, which may be of use in interpreting other Red Beds of the mid-continent of North America.

CHAPTER II

Geological Background

Geological Setting

Permian age rocks comprise the majority of Paleozoic rock units cropping out in western Oklahoma, the Texas panhandle and southwestern Kansas. The only exception is a thin veneer of late Miocene to Pliocene aged Ogallala conglomerates and sandstones, a few isolated outcrops of Cretaceous marine sandstones, and the Quaternary fluvial and eolian deposits associated with river courses of the tributaries of the Arkansas and Red Rivers. These Permian Red Beds are thought to represent the encroachment of a shallow epeiric sea from the west, which extended into the Delaware and Midland basins of West Texas and New Mexico to the southwest and similar shallow-epeiric seas of Kansas to the north (Hills, 1942; Holdoway, 1978; Johnson, 1990; Fig. 2). The area is bordered by the Wichita, Arbuckle, and Ouachita Mountains to the south and the Ozark Dome to the northeast (Fig. 2). Although there is an indication of tectonic deformation of Permian strata on the flanks of the Anadarko and Midland Basins, as well as local karsting in western Oklahoma, Texas and Kansas, deformation within the study area is minimal (Fay, 1962; Fay, 1964). Beds in west-central and northwestern Oklahoma have a gentle regional dip of 0.26 degrees to the southwest with local dips ranging between 0.07 and 0.37 degrees (Fay, 1964). Karst processes associated with some of the gypsum units and

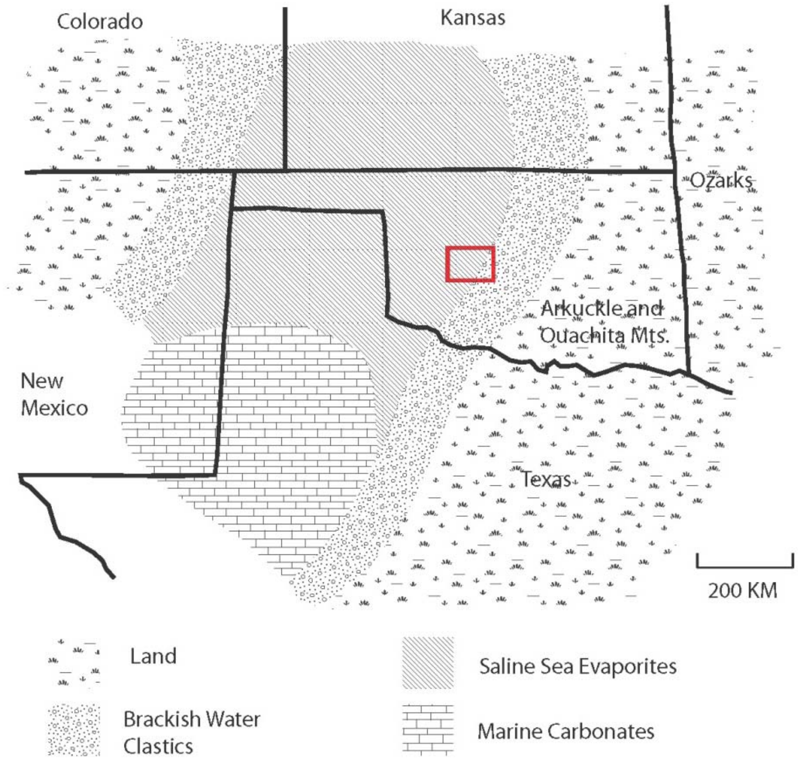

Figure 2- Paleogeographic map of the study area during during Blaine time. Modified from Johnson (1990). Red Box outlines approximate area of study.

other salt-related movements of some of the Permian beds have resulted in local deformation of the strata (Fay, 1962; Johnson, 1972; Gustavson *et al.*, 1980). Within the study area gypsum beds are at a minimal thickness and karst process are insignificant to nonexistent. A general stratigraphic column for the area is shown in Figure 3. The gypsum and dolomite beds within the Blaine Formation weather to produce prominent capstones creating the bluffs of the Blaine Escarpment and gypsum hills of western Oklahoma (Fig. 4). This provides an excellent setting to map the facies changes within the El Reno Group.

Geological Formations

Blaine Formation

Through correlations with equivalent strata in the Permian Basin of west Texas, biostratigraphy from bounding formations, and strontium isotope dating, the Blaine Formation is thought to be late Cisuralian or early Guadalupian in age (Clifton, 1944; Pendery, 1963; Fay, 1964; Johnson, 1967; Denison *et al.*, 1998; Fig. 3). Fay (1964) divides the Blaine Formation into three geographic units: a northern platform facies, a central basinal facies, and a southern deltaic facies. These depositional systems received sediment from both the Ozark Dome and the Ouachita and Arbuckle uplifts. Both the platform and central-basinal facies are comprised of alternating shales, dolomites and gypsums (Fay, 1964). The platform facies of the Blaine Formation have thicker gypsum beds but an overall thinner thickness than the basinal facies. The southern deltaic facies

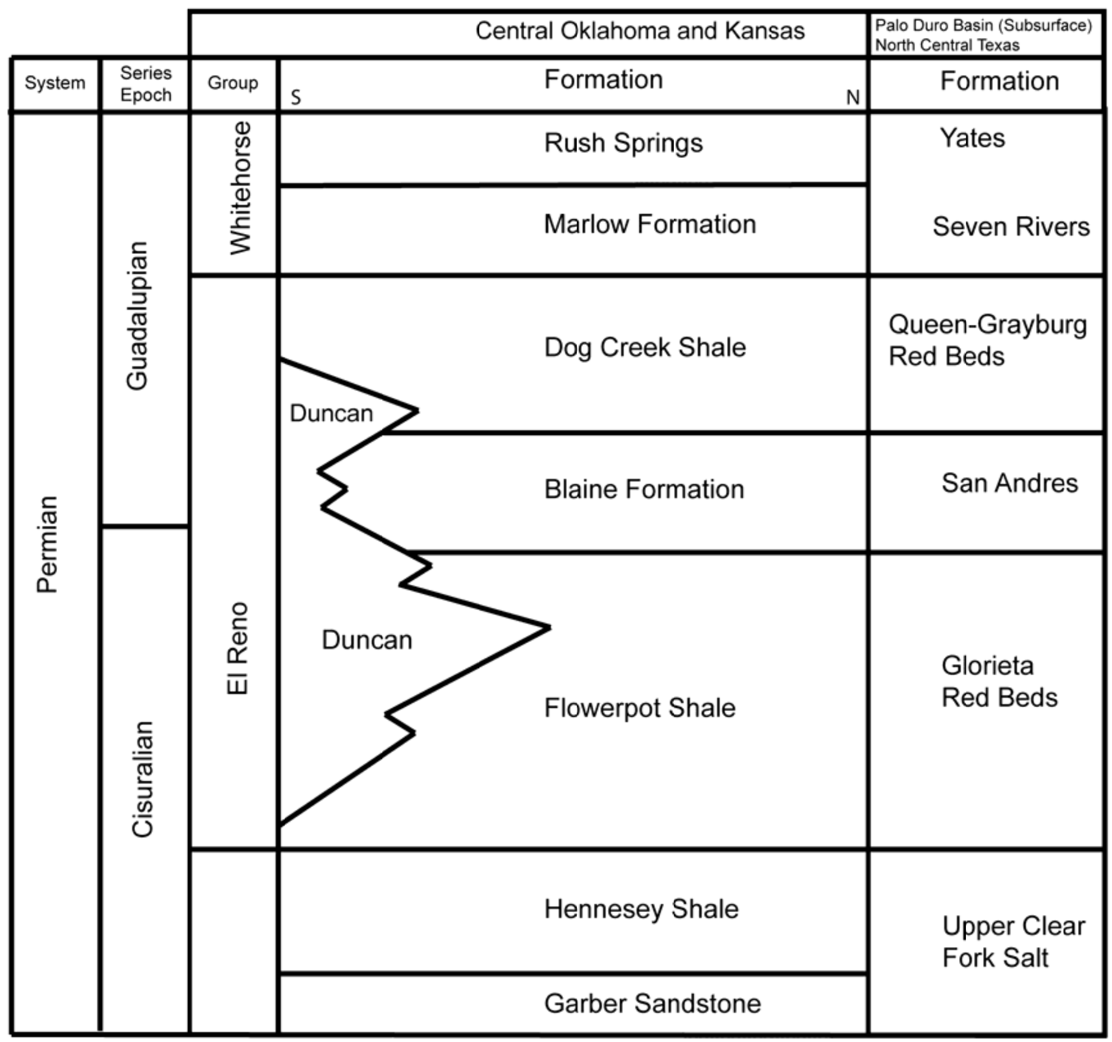

Figure 3-Simplified stratigraphic section of study area and equivalent units from the Palo Duro Basin (subsurface) and Kansas.

Figure 4- Typical escarpment of the Blaine Formation within the study area.

interfingers with sandstones and conglomerates of the Duncan Formation to the east and south (Fay, 1964; Fig. 5). As this change occurs the gypsum and dolomites disappear and the mudstone conglomerates and sandstones appear. This marks the change from the Blaine Formation to the Duncan Formation.

Previous authors have suggested that the gypsum-shale interbeds represent sea-level changes (Clifton, 1944; Fay, 1964). Fay (1964) concludes that when rivers flowing into the shallow sea were at a maximum seaward extent, with a more humid climate, the influx of siliciclastic material resulted in deposition of the shales of the Blaine Formation. Conversely the gypsum beds represent highstand times when the source of siliciclastic material is shifted further landward (Fay, 1964).

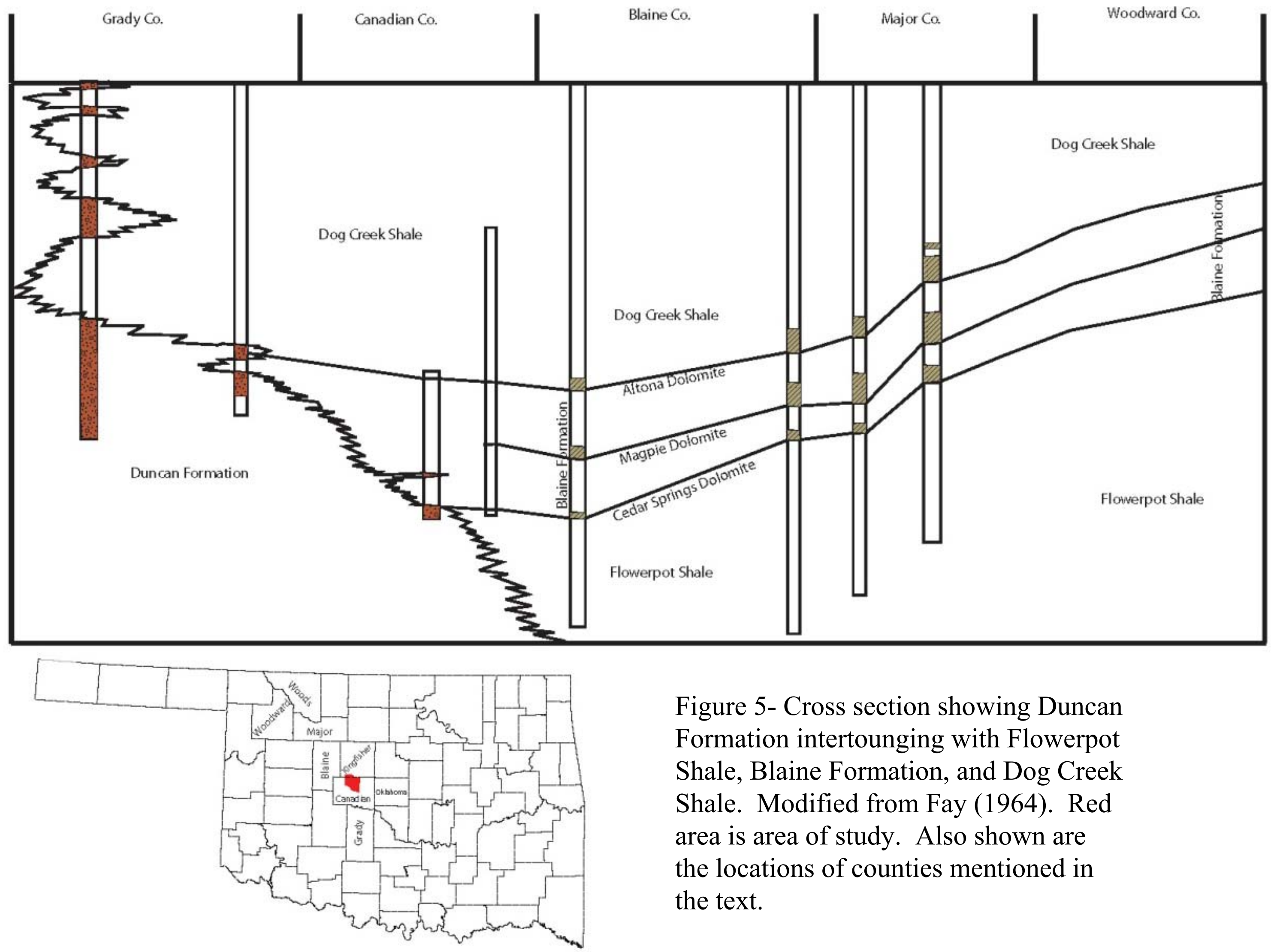

Figure 5- Cross section showing Duncan Formation intertounging with Flowerpot Shale, Blaine Formation, and Dog Creek Shale. Modified from Fay (1964). Red area is area of study. Also shown are the locations of counties mentioned in the text.

Duncan Formation

The Chickasha/Duncan Formation was known as the "purple sandstone", from the Purple Series, until Gould (1924) differentiated the Chickasha Formation from the underlying Duncan Sandstone. The description Gould (1924) gave of the Chickasha Formation came directly from Mr. Clyde Becker, and follows:

1. *An upper purple sandstone member 70 to 80 feet thick, the upper 30 feet of which consist chiefly of loose pink sand in which occur numerous thin lenses of purple "mudstone conglomerate" beds separated by thin strata of pink sand.*
2. *A middle pink sand member consisting of 50 feet of uncemented pink sand. Occasionally this sand shows cementation on both upper and lower contacts, but the lithologic characteristics are the same as of the pink sand, and not similar in texture or color to the "mudstone conglomerate."*
3. *A lower purple sandstone member chiefly composed of "mudstone conglomerates," 50 feet thick, more distinctly stratified than any other portion of the Purple Series.*

Recognizing that the Chickasha and Duncan Formation were similar in lithology, Sawyer (1924) considered the Chickasha and Duncan Formations as one formation that he termed the Duncan Sandstone. Green (1936) followed the terminology used by Sawyer (1924) and dismissed the name Chickasha Formation arguing that no unit described from the type locality could be traced. He instead grouped all formations from the "Purple Series" under the name Duncan Sandstone. The following year the name Chickasha was redefined, as separate from the Duncan Sandstone, for units that were found through most of Grady County (Brown, 1937). The Duncan Sandstone was considered a separate formation from the Chickasha Formation until Fay (1964) describes the character of the Duncan Sandstone (outside of the type section) to be the same as the Chickasha, and considered the two units as one.

The author of this paper, and others mapping the same units (e.g. Suneson and Stanley, 2001; Miller and Stanley, 2002) believe that the Chickasha Formation is indistinguishable from the Duncan Formation in outcrop and the two should be considered one formation. Since both names were introduced in the same paper (Gould, 1924) neither name has precedence over the other. Fay (1964) also considered the formations as the same, but failed to clear up the naming by referring to the units together as the Chickasha and Duncan Formation. This paper will follow the terminology used by Sawyer (1924) since he was the first author to use a single name to refer to all the units of sandstones, shales, and mudstone conglomerates as the Duncan Formation.

The Duncan Formation has been interpreted to be the proximal deposits that grade into the facies of the Blaine Formation, Flowerpot Shale, and Dog Creek Shale. These three units can be seen interfingering throughout central Oklahoma (Green, 1937; Fay, 1962; Fay, 1964; Fig. 5, Fig. 6).

Flowerpot Shale

Named for the type locality of Flower-pot Mound in Barber County, Kansas the Flowerpot Shale is a reddish-brown gypsiferous shale between the Medicine Lodge Gypsum of the Blaine Formation above and the Cedar Hills Sandstone below. The Flowerpot Shale has a maximum thickness of 142 meters and is divided into five lithologic units (Fay, 1964). Fay (1964) describes the Chickasha/Duncan Formation

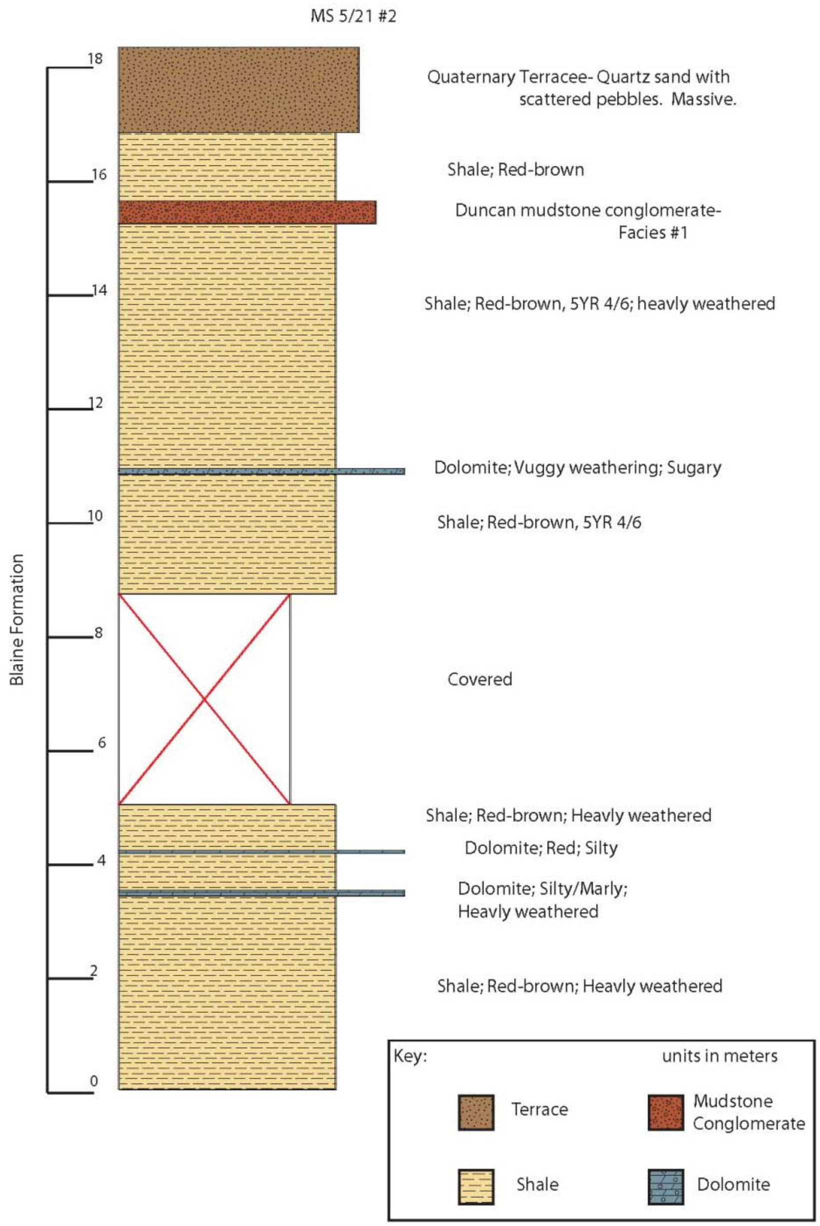

Figure 6- MS 5/21 #2. Measured section through the Blaine Formation. Note the Duncan mudstone conglomerate (Facies #1) incased in the Blaine Formation Shales.

interlayered with the Flowerpot Shale in Blaine County, Oklahoma. To the south in central Canadian County, it is believed that the Flowerpot Shale is represented by the lowermost Chickasha Formation (Fay, 1964).

Dog Creek Shale

The Dog Creek Shale is the name given to the series of reddish-brown clay shales with thin dolomites and siltstones between the top of the Altona Dolomite of the Blaine Formation and the base of the Marlow Formation (Fay, 1964). The Dog Creek Shale thins to the north from a thickness of 58 meters in Blaine County, Oklahoma to 9 meters in Kansas (Fay, 1964). The Dog Creek Shale contains several distinct dolomite and gypsum beds that have been used for correlation between Blaine County, Oklahoma and the type section in Kansas (Fay, 1964).

CHAPTER III

METHODOLOGY

The study includes the area between approximately 97° 55′ 00″ and 98° 7′ 30″ W and between the North Canadian River to the south and the Kingfisher/Canadian County border to the north (~35° 43′ 32″ N) (Fig. 7). This encompasses an area of approximately two 7.5′ quadrangles, and includes portions of four USGS topographic quadrangles: El Reno, OK; Fort Reno, OK; Fort Reno NE, OK; and Okarche, OK (Fig. 7). Topographic maps of the area were used as a basemap for geological mapping. For field work hard copies of the topographic maps were purchased from the Oklahoma Geological Survey. Geological mapping was conducted by driving sections roads and following stream traces over the entire study area. Digitizing of the geological map was done in the lab using ArcMap with the topographic maps as a base. Digital copies of topographic maps were downloaded from the Center for Spatial Analysis operated by the University of Oklahoma.

Rock samples were collected at various locations across the study area for thin section analysis and XRD analysis. Three samples were collected for thin sections from the Altona Dolomite (samples: 1/13 #1, 1/13#2, 1/13 #3) and two smaples from the Magpie Dolomite (samples: 2/6 #7, 2/6 #17) for comparison of the dolomite beds at different locations. Eight samples were collected for thin section analysis from the

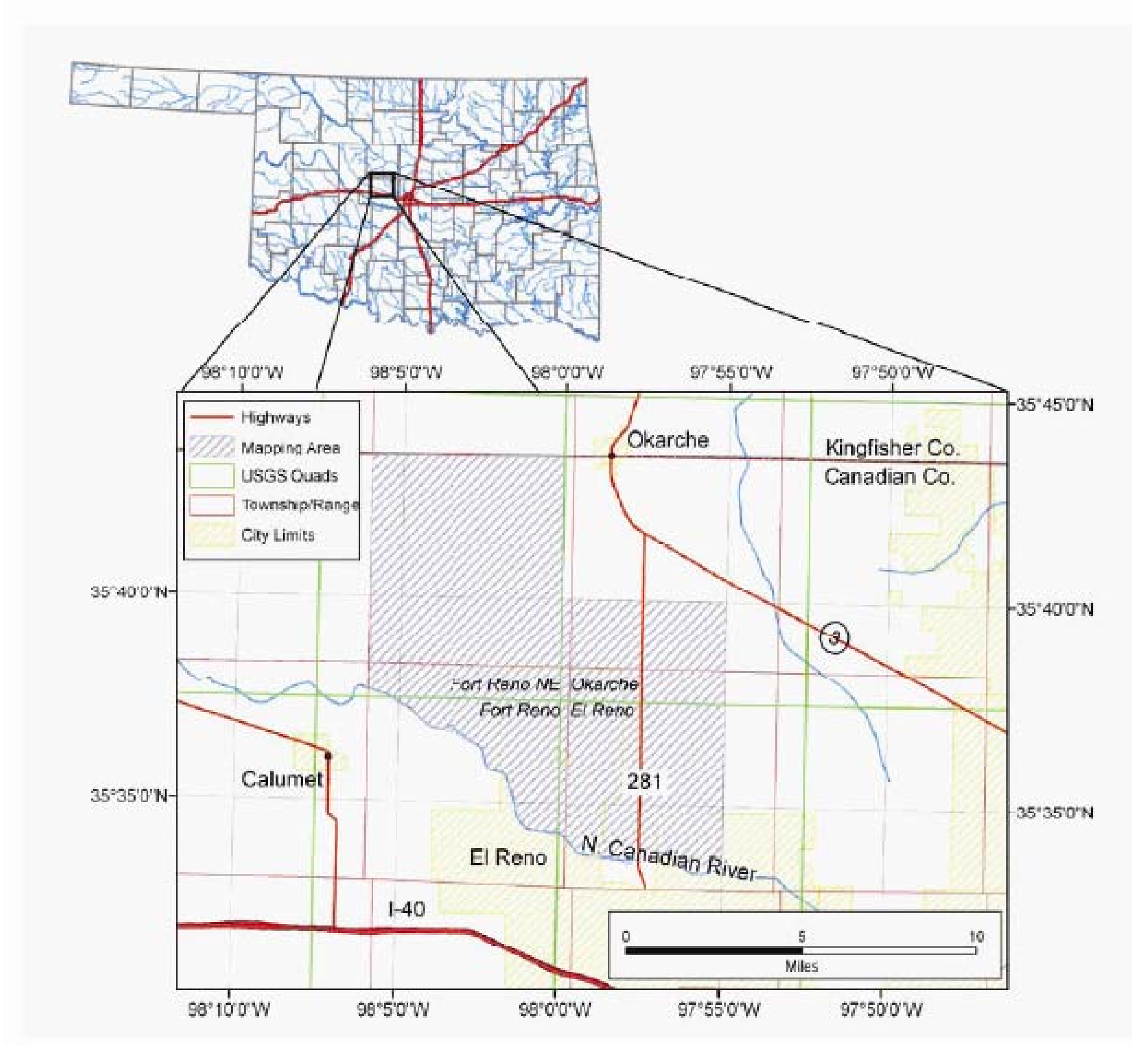

Figure 7- Location of mapping area. Four italiced names in center if inset map are the names of the respective USGS 7.5' quadrangles.

Duncan Formation for aiding in the description and interpretation of facies (samples: facies #1, 2/6 #1, 2/6 #20; facies #3, 2/6 #9, 2/6 #10, 2/6 #11; facies #4 2/6 #3; facies #6, 2/6 #2, 2/6 #12). Thin section analysis included point counts on all samples. Shale samples were taken from the Duncan Formation, Blaine Formation and Flowerpot Shale for XRD anyalsis. Six shale samples were collected from the Blaine Formation; two samples five to ten meters above the Blaine/Flowerpot contact, two samples one to three meters below the Magpie Dolomite and two samples one to three meters below the Altona Dolomite. These samples were taken at the western and eastern edges of the study area. Three samples were taken from the Flowerpot Shale at different locations across the study area. Two samples were taken from shales within the Duncan Formation.

Six locations were selected for measured sections. At those locations eleven sections were measured and described in detail. Two sections cover most of the Blaine Formation at locations at opposite (east-west) ends of the study area. One section was measured in the lower section of the Flowerpot Shale near the Flowerpot/Duncan contact. Eight sections were measured in the Duncan Formation for comparison of the different facies of the Duncan Formation (Fig. 6, Fig. 8, Fig. 9, Fig. 10).

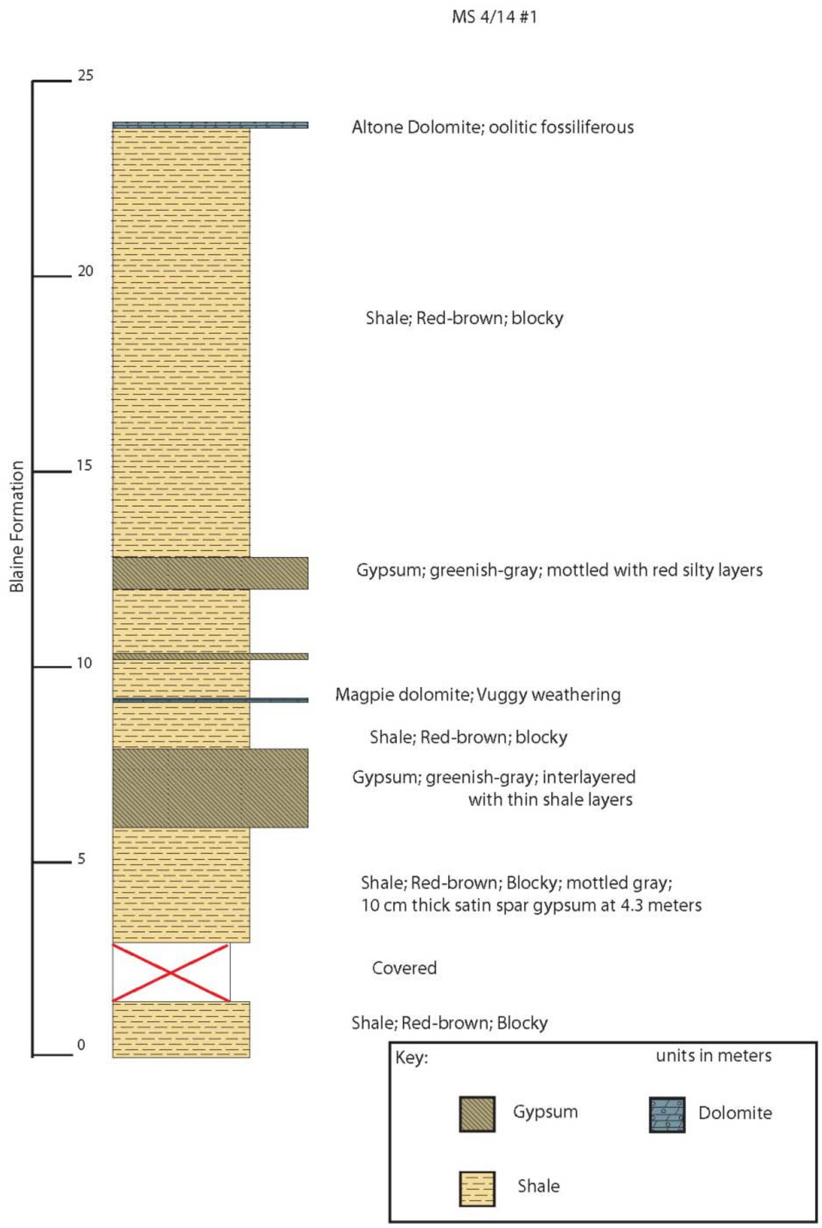

Figure 8- MS 4/14 #1. Measured section through Blaine Formation.

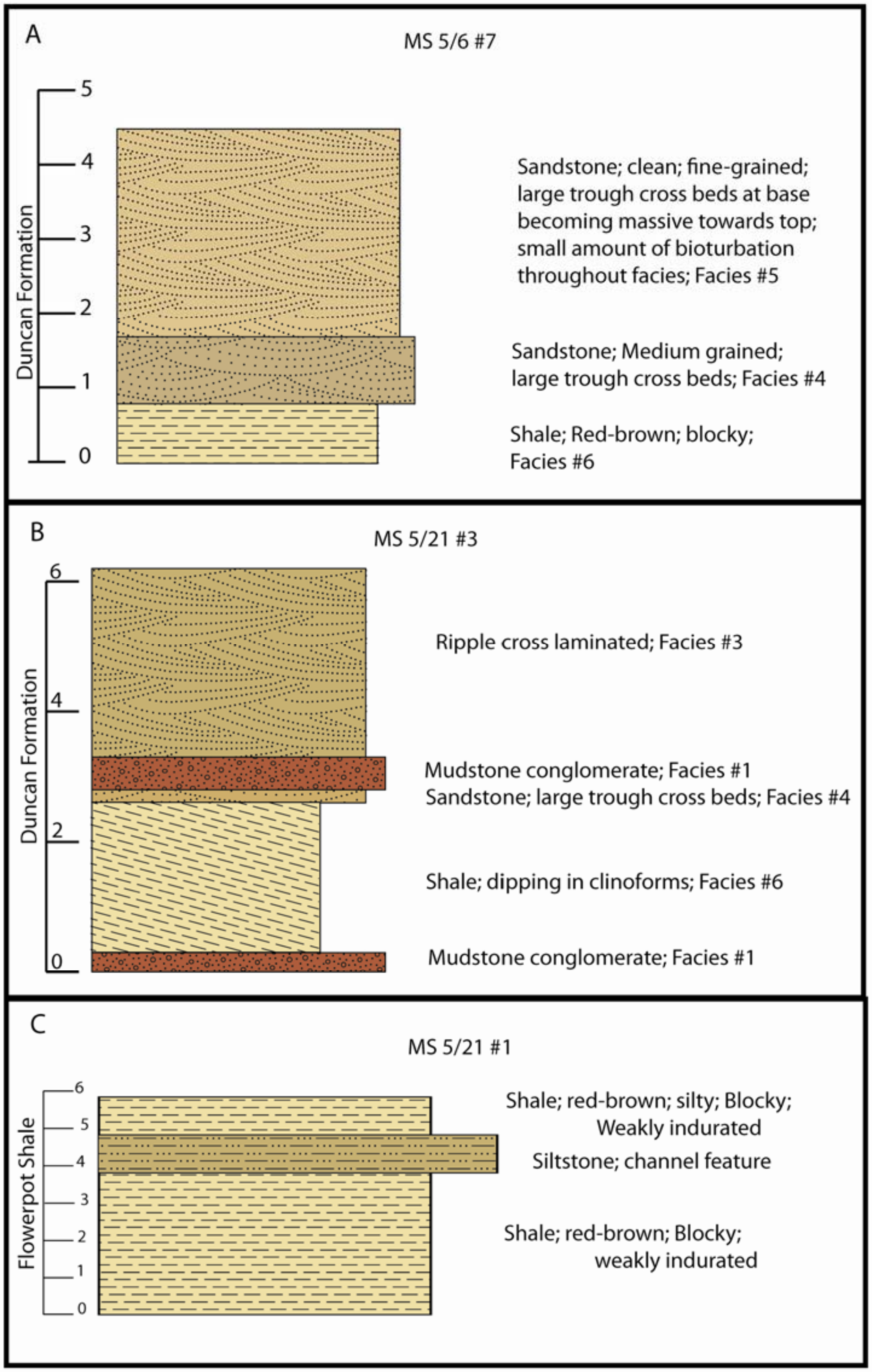

Figure 9- Measured sections. A) MS 5/6 #7. Duncan Formation; B) MS 5/21 #3. Duncan Formation; C) MS 5/21 #1. Flowerpot Shale.

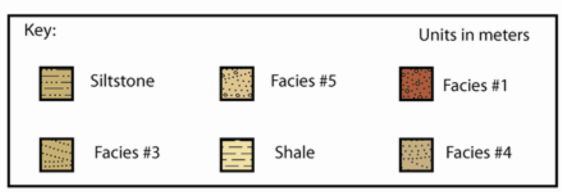

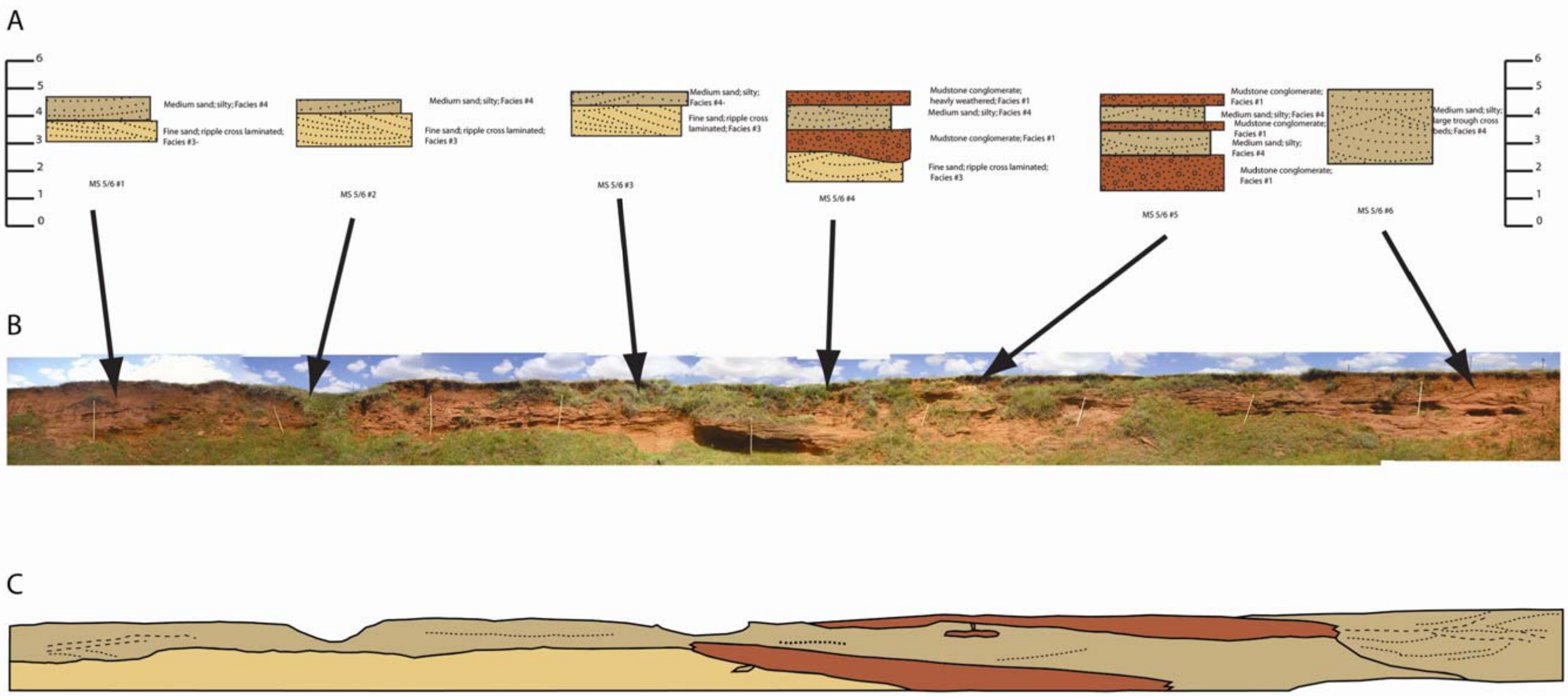

Figure 10- A) Measured sections from Duncan Formation in study area; B) Outcrop photo; C) Diagram showing facies that are present in outcrop.

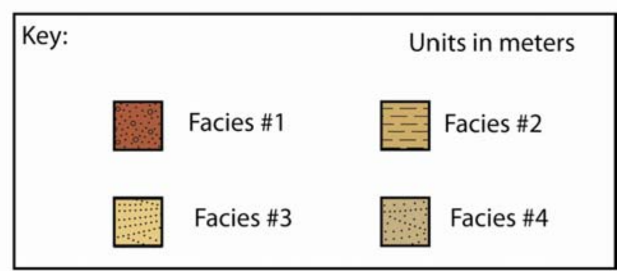

CHAPTER IV

RESULTS

Geological Map

A geological map at the 1:24,000 scale was produced for the study area (plate #1). Regional dip in the area is to the southwest, therefore younger units cropout to the southwest. Quaternary alluvial sediments, terrace deposits and dune sands are present in the southern portion of the study area. The Duncan Formation covers the largest area. The Duncan Formation is present in the north and northeastern portions of the map. Stratigraphically above, laterally equivalent and grading into the Duncan Formation are the Flowerpot Shale, Blaine Formation and Dog Creek Shale (Fig. 5). This is illustrated on the geological map as a thinning of the Flowerpot Shale, Blaine Formation, and the Dog Creek Shale to the southeast (plate #1).

Measured Sections

A complete description of the eleven measured sections from the study area can be found in Figures 6, 8, 9, and 10. Within MS 5/21 #2 the Duncan Formation facies #1 was found to be intertounging with Blaine Formation shales above and below (Fig. 6).

Quaternary Sediments

A thin veneer of Quaternary fluvial and eolian deposits associated with major river courses is found in the southern portion of the study area. Alluvial sediments of the North Canadian River flood plain cover the southern-most portion of the study area. Older alluvial terrace deposits are found to the north of the modern floodplain. Above these deposits recent sand dunes have developed along the western edge of the fluvial terrace. These dunes are no longer active, but were presumably developed at a time in the past when conditions were more arid (Brady, 1989; Muhs and Wolfe, 1999).

El Reno Group

Flowerpot Shale

Outcrops of the Flowerpot Shale are red-brown (2.5 YR 4/6) and clay dominated. Scattered silt and very fine sand units are also present in the Flowerpot Shale stratigraphically above the Duncan contact. These silty units are indications of the inter-tonguing of the Duncan Formation with the Flowerpot Shale.

Blaine Formation

The Blaine Formation consists of shales and interbedded gypsums and dolomites. These gypsum and dolomite beds form capstones that create the distinct escarpment of the Blaine Formation in Western Oklahoma (Fig. 4). Of the three named dolomite beds and four named gypsum beds of the Blaine Formation identified by Fay (1964), only two dolomites and three gypsums are present in the study area. The other units described by Fay (1964) are found to the west of the study area. The dolomite beds found include the

Altona Dolomite and the Magpie Dolomite. The gypsum members in the area include the Medicine Lodge Gypsum, the Kingfisher Creek Gypsum and the Nescatunga Gypsum. The Shimer Gypsum is found west of the study area. The gypsum units are only found in the northwestern part of the study area and the dolomite beds thin considerably to the south and east.

Dolomites

Altona Dolomite

The Altona Dolomite forms a well defined scarp from the northwest edge of the study area and continues to where the Blaine Formation grades into the Duncan Formation. The Altona Dolomite is oolitic and fossiliferous both in hand sample and thin section (Fig. 11a and Fig 11b). In outcrop the Altona Dolomite is gray to white in color. Fossils of the Altona Dolomite have a low diversity containing only a single genus of clam, *Permophorus* (Fay, 1964).

The majority of the Altona Dolomite is dolomitized micrite (52% avg.). Ooids and fossils were found in two of the three thin section samples (1/13 #1 and 1/13 #2). Secondary calcite cement is found in two samples (1/13 #2 and 1/13 #3). Porosity makes up the remainder of the samples and averages of 6.8%. The majority of the Altona Dolomite is an oolitic fossiliferous wackestone with a few local areas of oolitic fossiliferous packstone (Dunham, 1962). Petrographically the Altona Dolomite is fine grained with rhomb sizes ranges of 5 to 20 μm (Fig. 11c). The texture of the dolomite is planer-S (Sibley and Gregg, 1987).

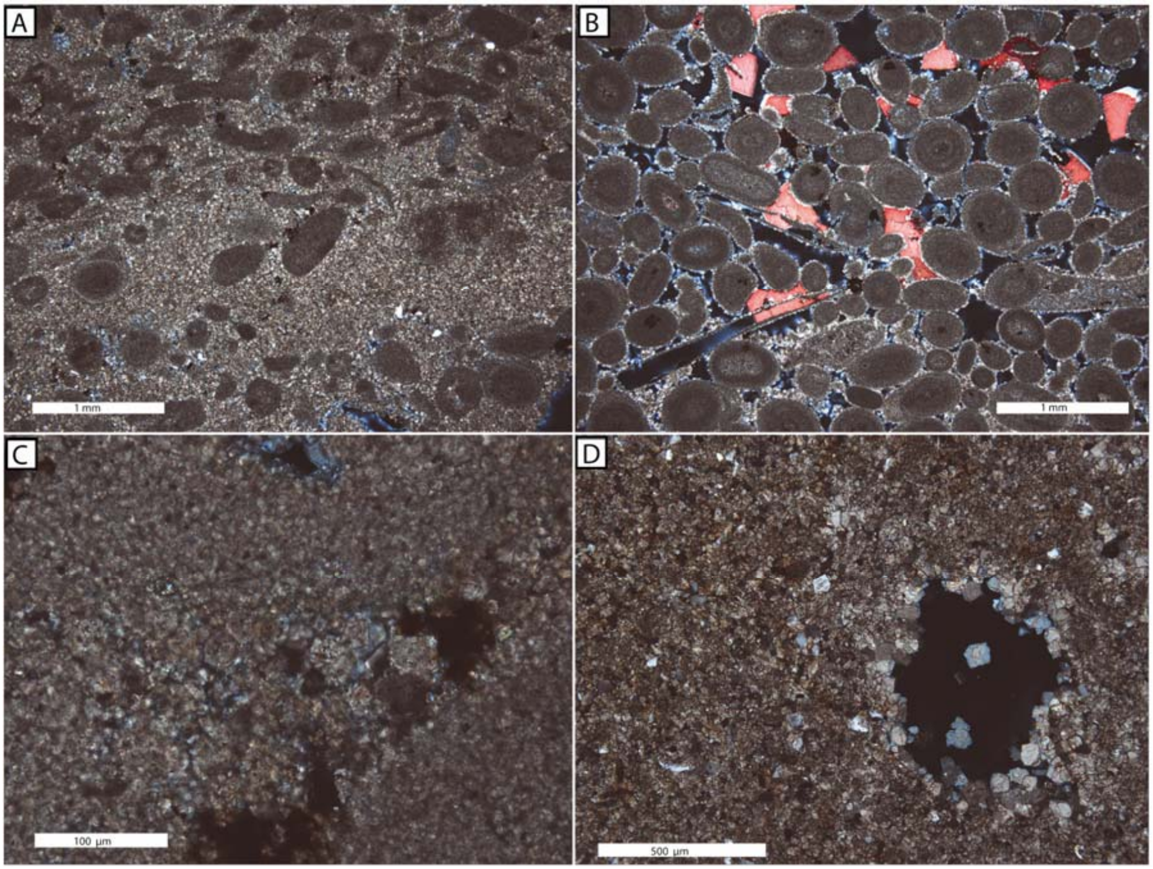

Figure 11- A. Altona Dolomite oolitic wackestone, 4x; B. Altona Dolomite oolitic fossiliferous packstone, 10x. Secondary calcite is stained red with alizarin red-S; C. Altona Dolomite showing rhomb size and texture, 40x; D. Magpie Dolomite, 10x.

Magpie dolomite

The Magpie Dolomite is not as well defined as the Altona Dolomite, but still forms a well defined scarp in the study area. The Magpie Dolomite is in most areas a silty fine crystalline dolomite that weathers into a distinctive vuggy texture (Fig. 12). This texture is helpful for field identification of the Magpie Dolomite. This vuggy texture comes from weathering of interlayered clays and silts in the dolomite. The color of the Magpie Dolomite is gray-reddish brown. Thin section analysis reveals that the majority of the Magpie Dolomite is fine crystalline dolomite (86%) with rhomb size ranges of 5-15 µm (Fig. 11d). Quartz grains represent 5% of the Magpie Dolomite. The quartz grains are on average silt-size (0.04 mm). Hematite cement (6%) and hematite grains (>1%) are also present in the Magpie Dolomite. Porosity values of the Magpie dolomite were lower than the Altona Dolomite at 3%.

Gypsums

The Medicine Lodge Gypsum member of the Blaine Formation was only found in one outcrop in the study area. The Medicine Lodge Gypsum consists of interbedded red shales and thin layers of nodular and satin spar gypsum. The Medicine Lodge Gypsum marks the contact between the Blaine Formation and the Flowerpot Shale. The Kingfisher Creek Gypsum is the thickest gypsum in the study area. In much of the western part of the study area the Kingfisher Creek has been mined and largely removed for aggregate material. The member is white, argillaceous, and mottled pink. The Kingfisher Creek forms a small escarpment throughout the study area. The Nescatunga Gypsum Member is present in the western part of the study area as a greenish-gray, argillaceous nodular gypsum. In some areas white-pink satin spar gypsum is interbedded

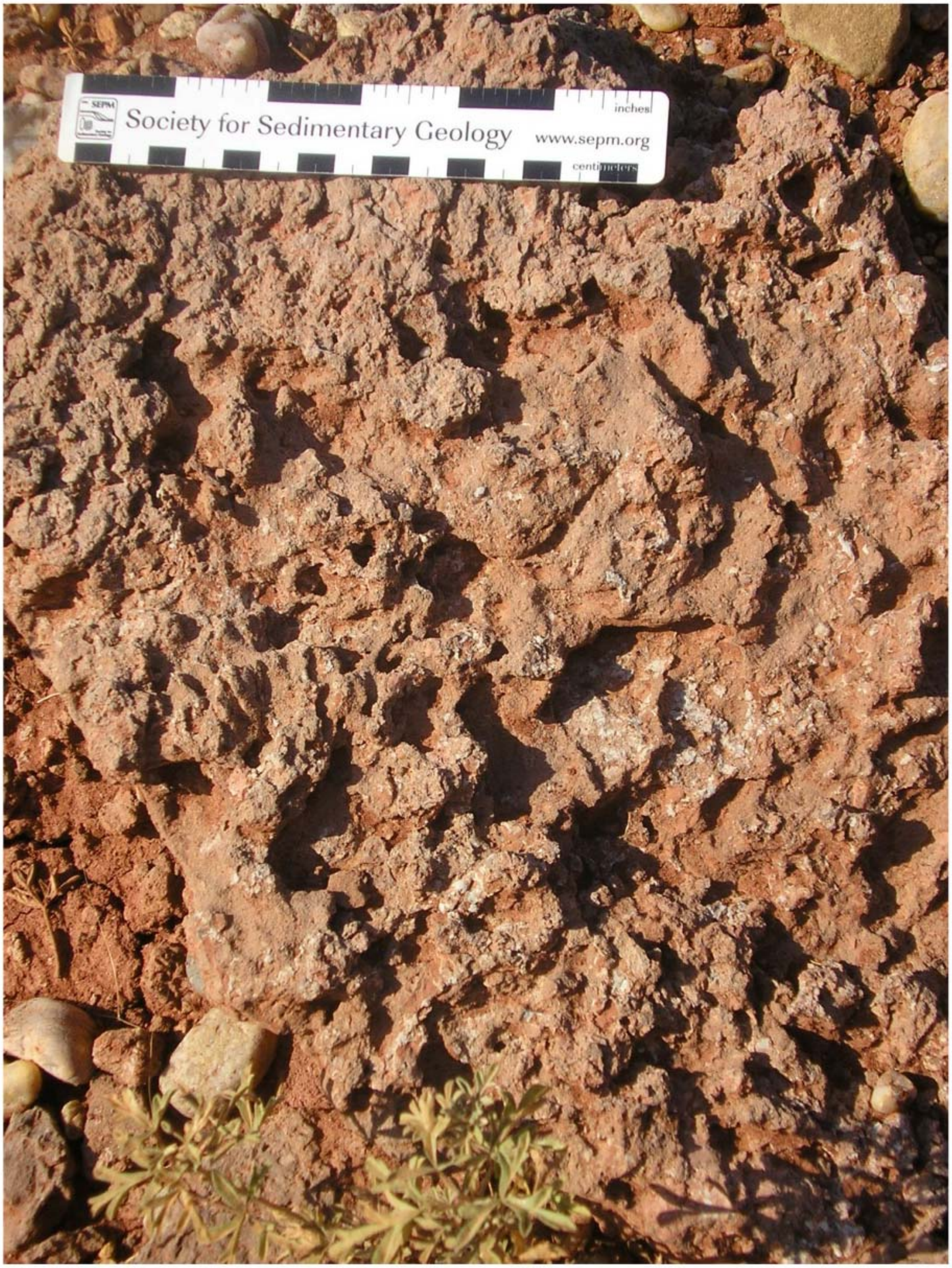

Figure 12- Magpie Dolomite. Note Vuggy texture.

with the green-gray unit. The Nescatunga is the first gypsum above the Magpie Dolomite.

Shales

Shales of the Blaine Formation are red-brown (5 YR 4/6) in color and blocky. Numerous mottled greenish-gray (gley2 8/10G) silty areas that display a channel-like geometry are present in Blaine Formation. These scattered silt layers are similar to those observed in the Flowerpot Shale.

Dog Creek Shale

The Dog Creek Shale consists of dark red (2.5 YR 3/6), blocky and fissle shales overlying the Altona Dolomite bed of the Blaine Formation. In the study area the Dog Creek Shale contains one minor silty dolomite layer and one to two scattered gypsum layers. Shales from the Dog Creek are darker red in color when compared to the shales of the Blaine Formation and the Flowerpot Shale.

Duncan Formation

The Duncan Formation contains interlayered sandstones, siltstones, mudstones, and mudstone conglomerates. Six major facies were identified within the study area based on grain size and sedimentary structures. The facies of the Duncan Formation are discontinuous and correlation from one outcrop to another outcrop is not possible.

Facies #1-Mudstone Conglomerate

The most distinctive facies of the Duncan Formation is the mudstone conglomerate facies. The thickness of the mudstone conglomerate beds are typically between 0.5 and 0.7 meters. The mudstone conglomerates of the Duncan Formation are generally found directly overlying sandstones, mudstones, and siltstones of Duncan facies #6, #3, or #4 and truncate underlying beds (Fig. 13a). The mudstone conglomerate facies grade laterally into medium and fine-grained sandstones of Facies #3 and #4 (Fig. 9).

Thin section analysis shows that sedimentary rock fragments make up the majority of facies #1 (average 39%). Average size for the rock fragments is 1.0 mm (very coarse sand), but some clasts are as large as 2.25 mm (gravel). The grains comprising the clasts are the same size and type as the matrix of facies #1. Two cements are present in Duncan facies #1, dolomite and hematite. Dolomite matrix comprises about 30% of the rock. Hematite cement is grain coating and makes up approximately 11% of the samples. The matrix of facies #1 is made of sand-size grains and clay. Sand grains make up 8% of the samples and the clay fraction comprises approximately 5% of the rock. The majority of the grains are quartz, but a small fraction of hematite grains were also observed. Porosity values for facies #1 average 4%.

Facies #2- Clay layers

Many scattered silty-clay layers were observed in the study area (Fig 13b). These clay layers were associated with other facies of the Duncan Formation. The clay layers are interbedded with deposits of Facies #3 and #4. Facies #2 is reddish-brown in color

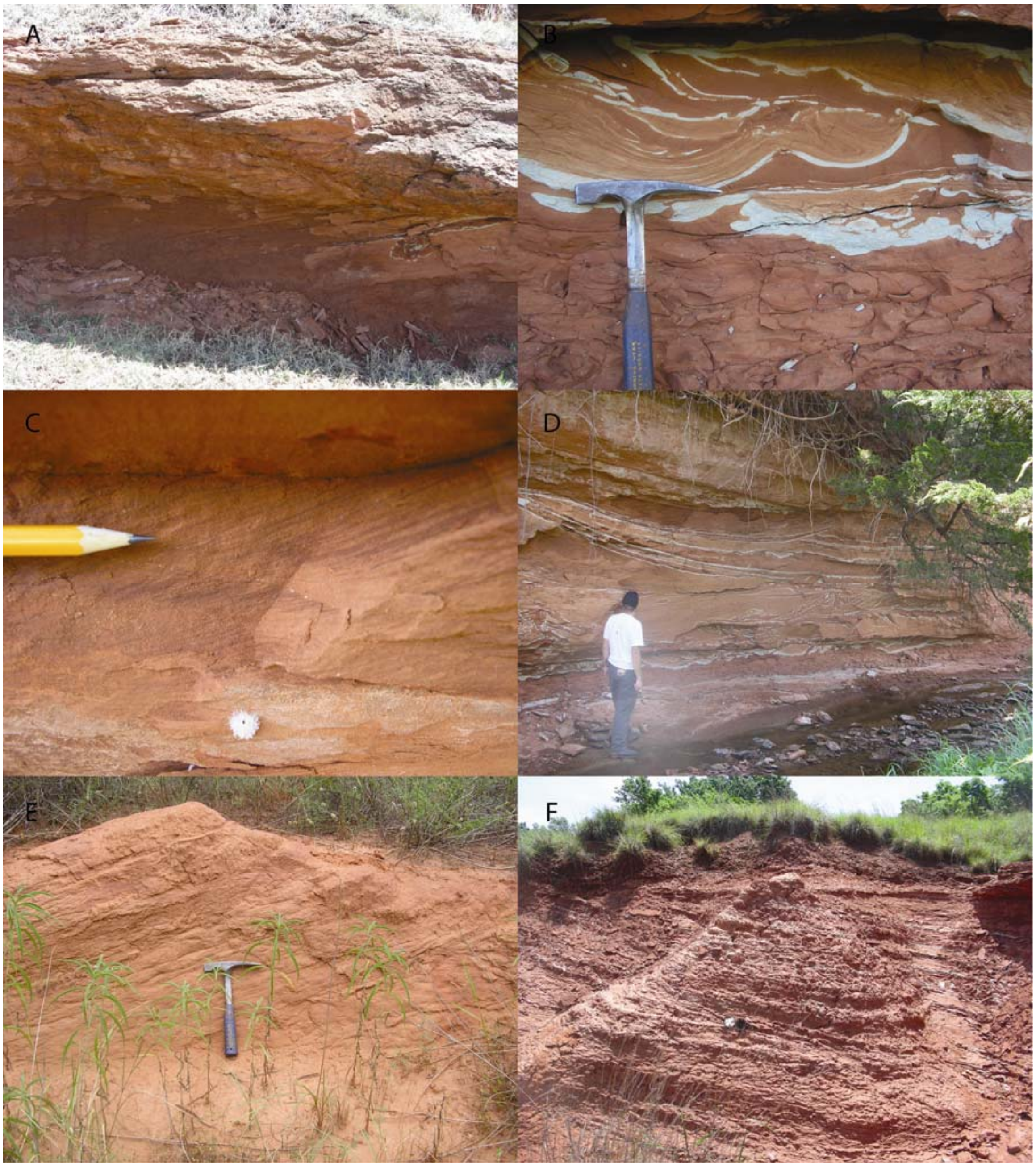

Figure 13-A) Facies #1. Mudstone Conglomerate showing erosional base with underlying Duncan shales; B) Facies #2. Diagenitic reducing zones highlighting silty-clay layers. Note convoluted bedding; C) Facies #3. Ripple cross laminated sandstone with interlayered clay drapes; D) Facies #4. Fine to medium grained sandstone with large scale low angle trough cross beds; E) Facies #5. Well sorted sandstone with high angle trough cross beds; F) Facies #6. Shale dipping in clinoforms.

and their thickness ranges from 10 to 30 cm. Convoluted bedding was observed between Facies #2 and Facies #4 (Fig. 13b).

Facies #3-Ripple cross laminated very fine-grained sandstone

The most abundant facies of the Duncan Formation in the study area is a very fine-grained ripple cross-laminated sandstone (Fig. 13c). The thickness of facies #3 is between 0.4 and 1.5 meters. Interlayered with the ripple cross laminated very fine sand layers are thin scattered drapes of fine grained silt and clay (Fig. 13c).

Thin section analysis of facies #3 shows that the majority of the constituents are quartz sand grains (54%). Hematite grains (avg. 5%) and volcanic rock fragments (avg. 6%) are also present. The average size of the grains is very fine sand with some grains up to 0.8 mm (coarse sand). Grain coating hematite cement is also present averaging 12% of the rock. Facies #3 has a relatively high porosity of 19%.

Facies #4-Fine to medium sand with large scale low angle trough cross beds.

Facies #4 contains large scale low angle trough cross beds (Fig. 13d). The thickness of this facies ranges from one to 3 meters. Facies #4 has an erosional base and overlies the red-brown blocky silty shale of the Duncan Formation (Facies #6). Scattered through Facies #4 are many discontinuous silty-clay layers of Facies #2.

In thin section, Facies #4 is shown to have a large fraction of clay matrix (Fig. 14). This facies consists mainly of quartz sand grains (avg. 30%) with an average size of 0.1 mm (very fine sand). Minor amounts of feldspars (3%), hematite (3%) and volcanic rock fragment (1%) are also present. Cements in facies #4 include

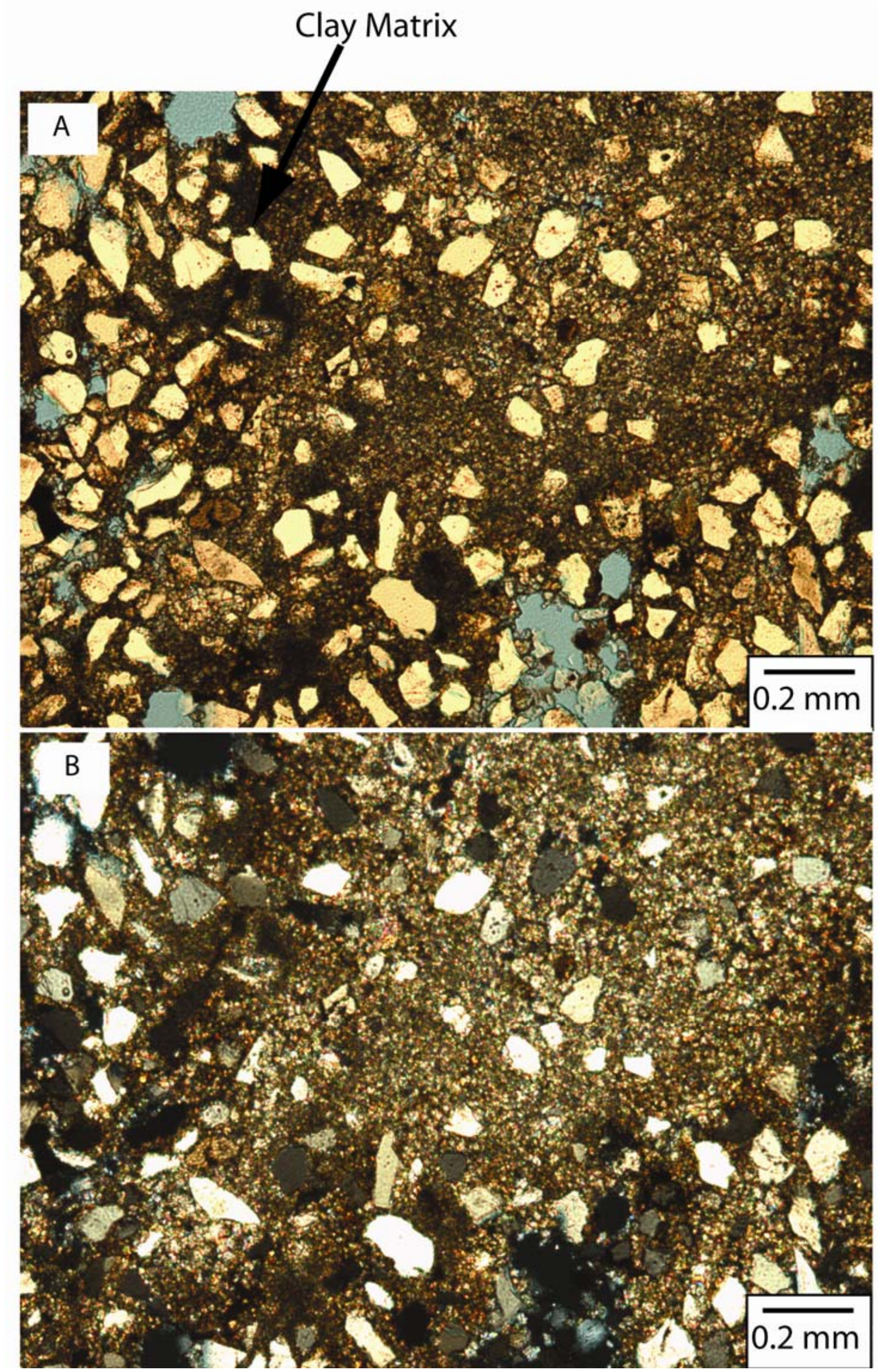

Figure 14- Facies #4 showing high fraction of clay matrix; A. Plain polarized light at 10x; B. cross polarized light at 10x.

calcite (26%) and grain coating hematite (3%). The large amount of clay matrix (28%) distinguishes this facies from other sandy Duncan Formation facies analyzed in thin section. Porosity values for facies #4 are similar to other facies at 7%.

Facies #5-Clean fine grained sandstone with high angle trough cross beds

Stratigraphically above Facies #4 is a well sorted fine grained sandstone (Fig. 13e). Numerous large scale high angle trough cross beds are present in the interval. The thickness of Facies #5 is at least 2.5 meters (Fig. 9a). The grain size of facies #5 ranges from fine to very fine sand. Facies #5 also contains many circular, burrow-like features lined with calcite glaebules (Fig. 15). These features are interpreted to represent root casts.

Facies #6-Shale/Mudstone

The fine-grained facies of the Duncan Formation is similar to the shale facies of related formations. The shale facies of the Duncan Formation often display a clinoform-like geometry (Fig. 13f). The modern (non-decompacted) dip on the clinoforms of facies #6 ranges from 12° to 14°. Red-brown shales and mudstones are seen in the field area stratigraphically below the mudstone conglomerates of Facies #1. Many reducing areas have a green-gray color. These color changes cut across shale laminations and are interpreted to represent diagenesis (Fig. 16). XRD analysis of the shales from the Duncan Formation reveal that they have a higher silica content than shales of the Flowerpot Shale and Blaine Formation (Table #1).

Figure 15- Circular burrow-like features from facies #5.

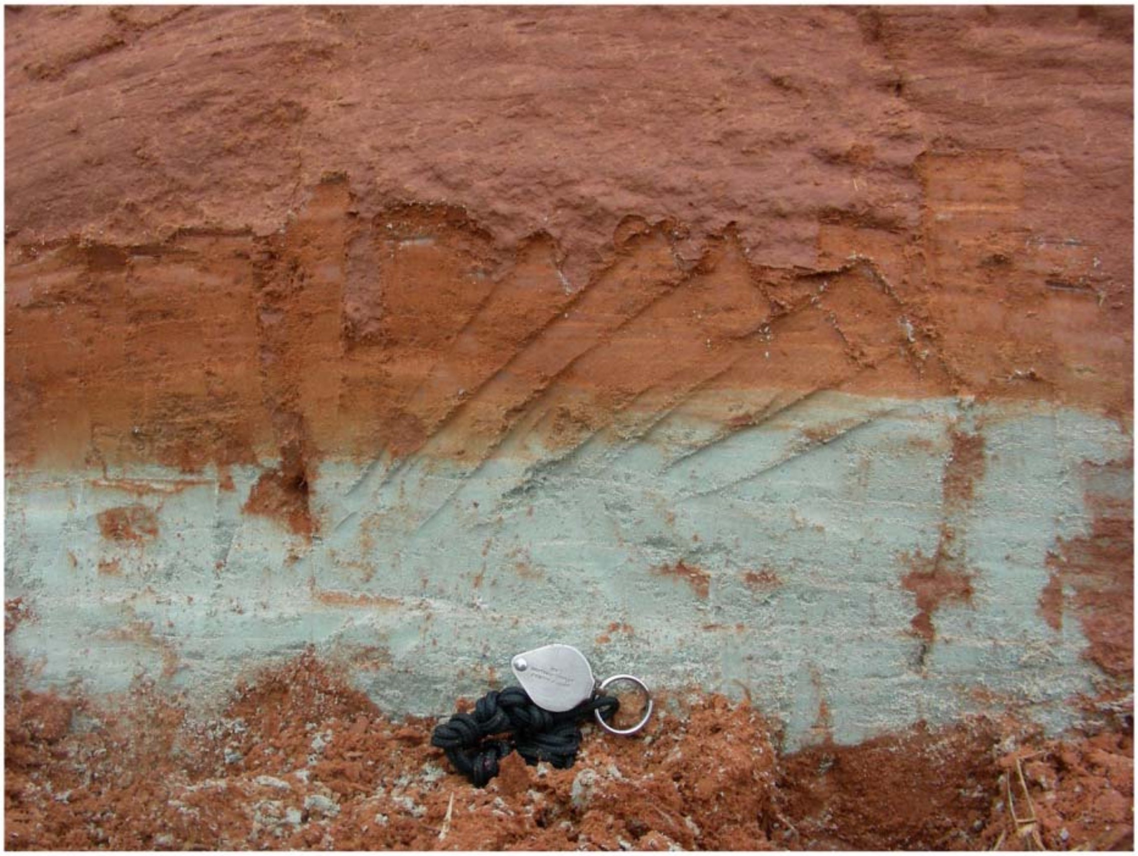

Figure 16- Diagenitic color change in the shales of the Duncan Formation. Reduced layer can be seen cutting across bedding layers.

Thin section analysis of facies #6 reveals that clay-size material is the most prevalent grain size of facies #6 (avg. 48%). Duncan facies #6 also contains a large amount of silt-sized (0.04 mm) quartz grains (33%). Small amounts of silt-size hematite grains (4%) and sedimentary rock fragments (2%) are also present. Cements in the Duncan facies #6 include calcite (1%) and hematite (3%). Porosity values on one of the samples are skewed because a large portion of the sample was lost during the grinding process, but values can be estimated at 4% for facies #6.

X-Ray Diffraction

X-ray diffraction (XRD) was conducted by Steve Chipera at Chesapeake Energy and a detailed description of the methods used can be found in appendix #1. Table 1 shows the normalized data from the XRD analysis. Illite is the major clay that is present in the El Reno group (Table #1), and illite values are consistent for all formations of the El Reno Group. Fay (1964) came to a similar conclusion. Quartz comprises the majority of the non-clay fraction with feldspar, hematite, calcite, dolomite, and gypsum also present in minor amounts (Table #1). Shale of the Duncan Formation differs from units of the El Reno Group with higher grain constituents and a lower clay fraction. This allows a distinction to be made between the shales of the Duncan Formation and shales of the other formations within the El Reno Group by comparing their quartz contents (Table #1). Intertounging of the Duncan Formation with the Flowerpot Shale is confirmed by XRD data. Sample 2/6 #19 taken from the Flowerpot Shale near the contact with the Duncan Formation has a higher quartz content than samples 2/6 #17 and 2/6 #18 taken stratigraphically lower in the section from the Flowerpot Shale (Table #1).

	Raw Data NORMALIZED to sum to 100%										
SAMPLE ID	#2	#12	#5	#13	#15	#6	#8	#14	#17	#18	#19
SAMPLE FORMATION	Duncan	Duncan	B/L	B/L	B/M	B/M	B/U	B/U	FP	FP	FP
NON-CLAY FRACTION											
Quartz	37.1	33.5	15.8	19.3	24.5	15.7	22.7	19.7	14.6	16.3	31.0
K-Feldspar	0.8	0.6	0.1	0.3	0.9	0.2	0.4	0.3	0.3	0.1	07
Plagioclase	10.9	10.1	4.5	6.2	7.8	4.7	6.2	4.5	5.2	4.5	8.6
Calcite	1.2	0.0	0.6	0.0	0.5	0.0	0.0	0.5	0.3	0.2	0.1
Dolomite	0.0	0.0	0.0	0.0	0.0	0.0	0.0	0.0	0.0	0.0	5.5
Gypsum	0.0	0.0	3.7	0.0	0.0	0.0	0.1	0.0	0.0	0.0	0.3
Hematite	1.7	1.5	1.6	2.6	1.7	1.6	1.5	1.8	1.8	1.7	1.5
TOTAL	51.8	45.7	26.3	28.4	35.4	22.2	30.9	26.8	22.2	22.9	47.7
CLAY FRACTION											
Mixed-Layer ILLITE/SMECTITE (Includes R3)	14.8	9.0	16.4	8.1	10.1	10.5	12.7	9.9	9.4	14.6	6.5
Illite + Mica	29.8	42.7	52.9	59.6	49.2	61.2	52.5	58.9	60.2	58.8	42.3
Chlorite	3.7	2.6	4.4	3.9	5.3	6.1	3.9	4.4	8.2	3.7	3.4
TOTAL	48.2	54.3	73.7	71.6	64.6	77.8	69.7	73.2	77.8	77.1	52.3
GRAND TOTAL	100.0	100.0	100.0	100.0	100.0	100.0	100.0	100.0	100.0	100.0	100.0
% Expandable Layers in I/S	17.8	17.9	18.0	18.1	18.9	19.7	19.8	20.9	19.8	17.8	19.1
% I/S to Illite in <1.0um Fraction	37.1	19.3	25.2	13.1	19.4	15.6	21.8	16.0	14.2	20.8	15.2
% Expandable I/S Layers in sample	2.63	1.61	2.95	1.47	1.91	2.07	2.52	2.07	1.86	2.60	1.25

Table #1- Table showing X-ray diffraction results. B/L -Blaine Lower. B/M- Blaine Middle. B/U- Blaine Upper. Fp- Flowerpot

CHAPTER V

DISCUSSION

Aridity

Clifton (1942) found several fauna within the Blaine Formation to the south and west of the study area. These faunas include ammonoids and nautiloids. However, other fauna usually associated with the observed cephalopods are absent, or poorly represented. Brachiopods, crinoids, and gastropods are extremely rare, and no fusulinids have been found within the Blaine Formation (Clifton, 1942). Boardman *et al.* (1984) and Kammer *et al. (1986)* have described a process by which dead cephalopods float into areas otherwise uninhabited by normal marine life. This process could explain the absence of brachiopods, crinoids, gastropods, and fusulinids with the presence of cephalopods within the El Reno Group.

Based on the thick gypsum deposits from the Blaine Formation, the absence of coals from a proposed marginal marine setting, the presence of dolomite (see Blaine and Flowerpot Depositional Environment), the absence of a normal marine fauna, and a low diversity of biota, the climate at the time of deposition of the El Reno Group is believed to have been arid. This arid environmental interpretation is supported by previous studies of the El Reno Group and equivalent formations (Fay, 1964; Presley, 1987; Johnson, 1990) as well as recent regional work (Tabor and Montanez, 2005; Peyser and Poulsen, 2008; Soreghan *et al.*, 2008a).

While the environment during the Permian is believed to have been arid it should be kept in mind that minor periods of more humid conditions may have existed. Work on Carboniferous strata in the Appalachian Basin point out that ongoing Milankovitch cycles will produce time periods of more humid climates during an overall arid time (Cecil, 1990; Cecil, 1996; Cecil and Edgar, 2003). These high-frequency changes explain the presence of flora and fauna indicating a humid climate from other Red Beds of the North American mid-continent (Olson, 1951; Olson and Mead, 1982).

Blaine and Flowerpot Depositional Environment

Working on Permian evaporites of the Texas panhandle equivalent in age to the El Reno Group, Presley (1987) identified four depositional environments. These include: 1) inner shelf, 2) brine-pan, 3) salt-flat, and 4) mud-flat. Presley (1987) interpreted the Flowerpot Shale and Blaine Formation of the Texas panhandle as an extensive supratidal mud-flat system characterized by interbedded red siliclastics. Presley (1987) drew upon mud flats from the Gulf of California (Thompson, 1968; Thompson, 1975) and Ranns of Kutch, India (Glennie and Evans, 1976) as analogues. Episodic flooding of these mud flats occurs during spring tides and strong storm surges. In addition, strong winds could produce water levels high enough to flood the entire region without large tidal ranges such as in the mud flats of Laguna Madre, TX (Fisk, 1959; Miller, 1975; Long and Gudramovics, 1983).

Handford (1981) conducted a study of the Clear Fork Formation (immediately underlying the San Andres Formation studied by Presley, 1987). He suggested that rocks, whose character is very similar to the Blaine Formation and Flowerpot Shale, are the deposits representing suspended material from discontinuous fluvial systems.

The amount of bromide within halite can sometimes be used to determine the origin and diagenesis of evaporites (Holser, 1966; Holser, 1970; Holdoway, 1978; Handford and Fredericks, 1980). Bromide concentrations between 50-200 ppm within halite are thought to indicate a marine origin (Holdoway, 1978). Typically, very low bromide concentrations (0-5 ppm) indicate that the salts were recycled by non-marine waters, or are not of marine origin (Holser, 1966; Holser, 1970). Bromide concentrations from the Flowerpot-Blaine salt have a concentration of less than 5 ppm Br^- (Holdoway, 1978). This supports an a nonmarine environmental interpretation for the Flowerpot-Blaine salt.

Strontium isotope values from the Blaine Formation in Blaine, County, Oklahoma suggest that the majority of the gypsums of the Blaine Formation have meteoric water contributions and do not necessarily represent open-water conditions (Denison *et al.*, 1998). Denison *et al (1998)* interpret the Nescatunga and Shimer Gypsums of the Blaine Formation to be sourced from open-marine waters, and the Medicine Lodge and Kingfisher Creek gypsums to have a significant meteoric contribution consistent with a mixed marine and terrestrial or fluvial source. Of the two gypsums interpreted by Denison *et al.* (1998) to be open-marine sourced (Nescatunga and Shimer), only one (Nescatunga) is present in the study area.

The Blaine Formation and the Flowerpot Shale contain several minor siltstone channels. These channels are scattered throughout the Blaine and Flowerpot section. These channels are interpreted to be the result of either: 1) frequent oscillations in sea level or 2) large discharge events associated with flooding of the surrounding lands resulting in flows reaching further into the basin. Similar channels were seen in the Upper Triassic Mercia Mudstone Group of west Somerset (England) (Talbot *et al.*, 1994). Presley (1987), recognized similar small scale channels within the Permian San Andres Formation (Blaine Formation equivalent) that he interpreted to represent minor terrestrial drainages.

The interbedded dolomite, gypsum and mudstones of the Blaine Formation have been interpreted to represent the result of changes in sea level (Fay, 1964). Fay (1964) noticed these cycles and interpreted the gypsums as representing highstands during arid times when clastic influx is lower, and the shales representing lowstands at more humid times when the clastic influx would be higher. Work on deposits from the Late Triassic of northwest Somerset (England) and the late Quaternary of east-central Australia suggest a different model. While the gypsums represent highstands, they also form at times when the environment is more humid and the mud-flats are periodically inundated in water (Talbot *et al.*, 1994). Shale deposition represents arid times when the mud-flats are exposed over much of the area (Talbot *et al.*, 1994). Widespread flooding of the mud-flats would result in environments suitable for the production of carbonates such as fossils and ooids. Evaporation of these waters would lead to gypsum and salt deposition. As the waters continue to withdraw, terrestrial clastics from the surroundings dominate. The reoccurrence of dolomite below gypsum capped by shales fit the Talbot *et al.* (1994) model. The classic flooding sequence for the Blaine Formation then would be represented by: 1) inundation of the area with lacustrine, possibly marine water resulting in the deposition of carbonate (dolomites), 2) evaporation of water to the point of gypsum deposition, and 3) mudstone deposition during periods of no water.

Within the study area the original calcium carbonate ooids and fossils from the Altona Dolomite and Magpie Dolomite have undergone complete conversion to dolomite. Several dolomitization models have been proposed for different units worldwide (Adams and Rhodes, 1960; Hanshaw *et al.*, 1971; Hsu and Schneider, 1973; Land, 1985; Tucker *et al.*, 1990). Based on the presence of evaporites in the Blaine Formation the models of dolomitization that best fit are those based on evaporation, i.e., evaporitic pumping (sabkha) or seepage-reflux. The evaporative pumping model for dolomitization was developed by studies of sabkhas in Abu Dhabi by Hsu and Schneider (1973) and (McKenzie *et al.*, 1980). This model invokes flooding of the sabkha by marine water leading to downward movement of water through sediments to form a net seaward flow of groundwater. Warm temperatures over the sabkhas leads to evaporation and an upward flow of ground water to the capillary zone. The seepage-reflux model is usually applied to ancient dolomites associated with evaporites (Adams and Rhodes, 1960; Fisher and Rodda, 1969). This model involves precipitation of gypsum in a shelf environment to raise the Mg/Ca ratio of the fluid. Then these Mg enriched brines descend through permeable strata below and replace less dense marine pore water causing dolomitization (Adams and Rhodes, 1960; Tucker *et al.*, 1990). These models for dolomitization are consistent with arid climate during the time of El Reno deposition. Petrographically, the majority of modern evaporative dolomite is fine grained with dolomite crystal rhombs ranging in size from 1 to 5 μm, and ancient dolomites thought to have formed by this mechanism have rhomb sizes ranging from 5 to 20 μm (Tucker *et al.*, 1990), consistent with the crystal sizes of the Altona Dolomite and Magpie Dolomite (Fig 11d).

Based on similar studies from the Texas panhandle (Presley, 1987), proposed evaporation models for dolomitization, bromide concentrations (Holdoway, 1978; Handford, 1981), strontium isotope ratios (Denison *et al.*, 1998), and observed siltstone channels (Talbot *et al.*, 1994), the author of this paper interprets the Blaine Formation in the study area to be the result of mud-flat deposition in a continental sabkha environment with sporadic inundation by lacustrine, or possibly marine waters.

Duncan Depositional Environment

Previous authors have always followed the interpretation of Green (1937) that the Duncan formation is a delta, even naming it the Tussey delta. Work on recent sediments of central Australia (Tooth, 1999; Lang *et al.*, 2004; Nichols and Fisher, 2007; Fisher *et al.*, 2008) and Permain to late Triassic deposits from the Solway Basin, United Kingdom (Brookfield, 2008) may provide a clearer understanding of the environment at the time of Duncan deposition. The association of coarse grained Duncan facies intertounging with supra tidal, continental sabkha, mud-flat facies of the Flowerpot Shale, Blaine Formation, and Dog Creek Shale indicate that the Duncan Formation may have been deposited in a different setting such as an alluvial fan, shoreline or terminal splay.

Terminal Splay Deposits

Recent work on Lake Eyre, central Australia has attempted to build a facies model for terminal-splay deposits (Tooth, 1999; Lang *et al.*, 2004; Nichols and Fisher, 2007;

Fisher *et al.*, 2008). Fisher *et al.* (2008) defines a terminal splay as – "a lobe-shaped body of sediment found at the terminus of a river that has been deposited from unconfined, sub-aerial sheetfloods which propagated over a dry floodplain, playa or lakebed." Fisher *et al.* (2008) defines a terminal splay complex as – "a large-scale, amalgamated sediment package which may include sediment deposited and reworked by both sub-aerial processes (e.g. fluvial, sheetflooding, aeolian) and sub-aqueous processes (e.g. deltaic) at the terminus of a fluvial system." Fisher *et al.* (2008) breaks the terminal splay into three parts: distributary channel, proximal splay, and distal splay.

The distributary channel is composed of bedload material deposits from confined flow. Cross-bedded and massive bedded sands and a significant amount of ripple-laminated sand dominate the sedimentary structures of the distributary channels. All of these structures may be associated with clay. Discontinuous layers of clay and gravel are also present in the distributary channel (Fisher *et al.*, 2008).

Deposits of the proximal splay are dominated by thick beds of planer cross-bedded and massive sands. The sediments are dominantly bedload material of clean, medium-grained to coarse-grained sands. Thin beds of ripple-laminated sands are also common and thin beds of clay line a few of the sandy lithofacies (Fisher *et al.*, 2008). Proximal splay deposits represent the initial stages of the flow leaving the distributary channel and becoming unconfined. Fisher *et al.* (2008) suggests that the initial stages of the flow becoming unconfined have an erosional component based of the presence of small erosional surfaces and large clay clasts.

Distal splay deposits are dominated by very fine-grained, massive sand. This sand lithofacies is intercalated with a clay lithofacies (Fisher *et al.*, 2008). Thinly bedded horizons of carbonaceous silt are commonly seen in the outer reaches of the distal splay. Fisher *et al.* (2008) suggest that these silt layers are the result of waning flow as the flood waters reach further into the basin. The absence of cross-bedding and ripple-laminations indicate that the sediments of the distal splay primarily represent suspended load. This dominance of suspended load sedimentation is what differentiates the proximal splay from the distal splay (Fisher *et al.*, 2008).

Comparison of Duncan Facies to Terminal Splay Deposits

The facies of the Duncan Formation identified in this study have similarities to the facies identified from arid terminal-splay deposits. Fisher *et al.* (2008) describes seven facies of modern terminal splays. Overall the splay deposits decrease in grain-size, thickness of the lithofacies, erosional surfaces and evidence of bedload sedimentary structures with increasing distance from the source. Table #2 is a summary of the lithofacies of Fisher *et al.* (2008).

Fisher's facies G_s is comparable to Facies #1 of the Duncan Formation (Table #2). Both facies are interpreted as channel deposits and have erosive bases. The Duncan Formation facies #1 is on average thicker with a thickness of 0.5 to 0.7 meters compared to 0.1 meter thickness of the G_s facies. This is most likely due to the splay of the Duncan Formation being larger in size than the Douglas Creek terminal splay of Fisher *et al.* (2008).

Facies S_r from Fisher *et al.* (2008) is equivalent to facies #3 of the Duncan Formation (Table #2). Facies #3 is the most abundant facies identified within the Duncan Formation. Ripple laminations and drapes of silt and clay were seen in both the Douglas

			Thickness (mm)				Grain-size (phi)					
	Lithofacies	Sedimentary Structures	Max	Min	Mean	Med	Max	Min	Mean	Med	Interpretation	Duncan-equivalent facies
Cl_m	Clay	Thin sharp, planar-based laminae	310	5	60	40	-	-	-	-	Deposition out of suspension from standing water	Facies #2
F_m	Silt, Clay	Massive, planar based, varying amounts of bioturbation	120	10	50	30	-	-	-	-	Deposition from low velocity flow, post-depositional pedogenesis	-
F_c	Carbonaceous Mud	Organic matter preserved in thin discontinuous beds, and lens deposits	15	5	10	10	-	-	-	-	Deposition of organic material and silt from low velocity flow	-
S_m	Sand, coarse to very fine	Massive, planar based unit often with high clay/silt component, sometimes fining up	550	5	80	50	0	3	2.3	3	Fluvially deposited sediments that have had primary sedimentary structure suppressed	-
S_r	Sand, Coarse to very fine with rare pebble	Asymmetric ripple cross-lamination	320	20	80	70	2	3	2.6	3	Ripples - bedload	Facies #3
S_c	Sand, coarse to fine with occasional pebble clasts	Planar and trough cross-bedding, sometimes fining up	340	40	130	110	1	3	2	2	Straight and sinuous crested bedforms – bedload Least mobile bedload	Facies #4
G_s	Clast-supported, crudely bedded gravel	Horizontal bedding, massive structure	100	10	20	20	-	-	-	-		Facies #1

Table 2- Summary of lithofacies from Fisher *et al.* (2008).

Creek splay and the Duncan Formation. The ripple laminations are believed to be the result of bedload deposition. As the flow is waning the finer grained silt and clay drapes are deposited (Ashley *et al.*, 1982).

The S_c facies of Fisher *et al.* (2008) consist of fine to coarse sand with occasional pebble casts. Structures identified by Fisher *et al.* (2008) include planer and trough cross-bedding. This S_c facies from Fisher et al. (2008) is comparable to Facies #4 from the Duncan Formation.

Contained within both Facies #3 and Facies #4 of the Duncan Formation are silty-clay layers of Facies #2. This Facies #2 is equivalent to the Cl_m facies of Fisher et al. (2008). These deposits are interpreted to represent deposition from suspension from standing water in small ponds formed on the terminal splay (Fisher *et al.*, 2008).

The S_m facies of Fisher *et al.* (2008) is a widespread massive facies with grain-sizes ranging from fine to coarse sand (Table #2). Fisher *et al.* (2008) identifies several potential causes for the massive structure of the S_m lithofacies. One of these causes is post-depositional bioturbation (Retallack, 1990; Talbot *et al.*, 1994). Bioturbation could explain why the S_m facies is not seen in the Duncan Formation. Bioturbation was seen in the study area at one location within Facies #5 of the Duncan Formation (Fig. 9a). Limited bioturbation in the study area could have helped to preserve primary structures that would have been destroyed had the study area been habitable to organisms during deposition.

Within the Duncan Formation the mudstone channels are seen stacked and are present at several locations throughout the study area (Fig. 10). These stacked channels indicate that the Duncan Formation is a terminal-splay complex rather than a single terminal splay (Fisher *et al.*, 2008). These channels appear to be found randomly throughout the section and no correlation was identified between their presence and either gypsum-rich or shale-rich intervals within the Blaine Formation and Flowerpot Shale.

As sediment is sourced from the east onto the mud-flat environment, the majority of bedload and coarse sand-sized material is trapped in the terminal-splays represented by the Duncan Formation. The higher amount of quartz (Table 1) from the Duncan Formation confirm earlier work from the Blaine Formation that showed the amount of quartz in samples of the El Reno Group decreases to the west (Blatt and Totten, 1981). Although, Blatt and Totten (1981) assumed that the Blaine Formation was a marine environment, the same distribution in coarse-grained clastics would be expected in a continental sabkha-like system. In lue of marine processes redistributing the coarser material basinward (west), eolian or occasional high-intensity floods could transport the material towards the west out onto the mudflats represented by the Blaine Formation and the Flowerpot Shale. Prevailing winds are thought to have been from a southeasterly direction by early Permian time (Dott and Batten, 1971; Soreghan and Soreghan, 2007; Soreghan *et al.*, 2008b). One would therefore expect decreasing amounts of sand as you move towards the center of the mudflats.

Through measured section and examination of different facies, it is believed that the El Reno Group was deposited in an arid continental sabkha setting. Figure 17 summarizes a model of how the facies within the El Reno Group were deposited on the edge of a Permian intracontinental basin.

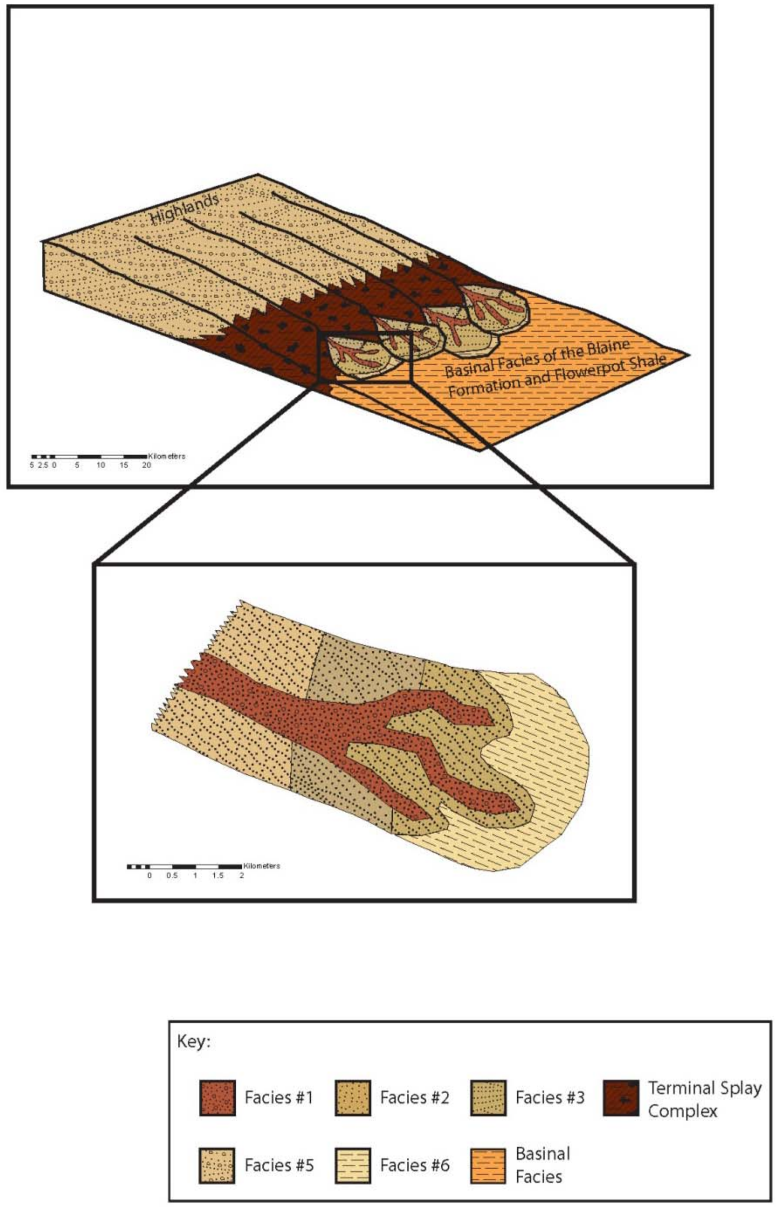

Figure 17- Facies model for the El Reno Group.

CHAPTER VI

CONCLUSION

Through geological mapping, measuring section, and analyzing thin sections and XRD data, the deposits of the El Reno Group (Permian) of central Oklahoma were examined. Based on similar studies from the Texas panhandle, proposed evaporation models for dolomitization, bromide concentrations and strontium isotope ratios from previous studies, and observed siltstone channels within the shales, the Flowerpot Shale, Blaine Formation, and Dog Creek Shale are interpreted to represent a continental sabkha environment with sporadic inundation by lacustrine, possibly marine waters. The classic flooding sequence for the Blaine Formation is represented by: 1) inundating the area with lacustrine or marine water resulting in the deposition of carbonate (dolomites), 2) evaporation of water to the point of gypsum deposition, and 3) mudstone deposition during periods of no water. Six facies were identified within the coarser-grained Duncan Formation: 1) mudstone conglomerate; 2) clay layers; 3) ripple-cross laminated very fine-grained sandstone; 4) fine to medium sand with large scale low angle trough cross beds; 5) clean fine-grained sandstone with high angle trough cross beds and root casts; and 6) shale-mudstone. These facies are similar to the facies described in the Douglas Creek terminal splay of Lake Eyre in central Australia and other terminal-splay deposits from Australia. This comparison supports an interpretation that the Duncan Formation was deposited on the edge of an intracontinental basin as a terminal-splay complex as defined by Fisher *et al.* (2008). Our work suggests that arid-land depositional environments may provide a better analogue when trying to interpret the Red Beds of the North American mid-continent than traditional depositional models.

REFERENCES

Adams, J.E. and Rhodes, M.L., 1960. Dolomitization by seepage refluxion. Bulletin of the American Association of Petroleum Geologists, 44: 1912-1920.

Andreason, M.W., 1992. Coastal siliciclastic sabkhas and related evaporative environments of the Permian Yates Formation, North Ward-Estes Field, Ward County, Texas. AAPG Bulletin, 76: 1735-1759.

Ashley, G.M., Southard, J.B. and Boothroyd, J.C., 1982. Deposition of climbing-ripple beds; a flume simulation, Sedimentology. Blackwell : Oxford-Boston, International, pp. 67-79.

Becker, C.M., 1930. Structure and stratigraphy of southwestern Oklahoma. Bulletin of the American Association of Petroleum Geologists, 14: 37-56.

Bhattacharya, J.P. and Giosan, L., 2003. Wave-influenced deltas; geomorphological implications for facies reconstruction. Sedimentology, 50: 187-210.

Blatt, H. and Totten, M.W., 1981. Detrital quartz as an indicator of distance from shore in marine mudrocks. Journal of Sedimentary Petrology, 51: 1259-1266.

Boardman, D.R., II, Mapes, R.H., Yancey, T.E. and Malinky, J.M., 1984. A new model for the depth-related allogenic community succession within North America Pennsylvanian cyclothems and implications on the black shale problem. Tulsa Geological Society Special Publication, 2: 141-182.

Brady, R.G., 1989. Geology of the Quaternary dune sands in eastern Major and southern Alfalfa counties, Oklahoma, United States.

Brookfield, M.E., 2008. Paleoenvironments and Paleotectonics of the arid to hyperarid intracontinental latest Permian- late Triassic Solway basin (U.K.). Sedimentary Geology 210: 27-47.

Brown, O.E., 1937. Unconformity at base of Whitehorse Formation, Oklahoma [with discussion by Henry Schweer and Hastings Moore]. Bulletin of the American Association of Petroleum Geologists, 21: 1534-1556.

Cecil, C.B., 1990. Paleoclimate controls on stratigraphic repetition of chemical and siliciclastic rocks. Geology [Boulder], 18: 533-536.

Cecil, C.B., 1996. Climatic controls on Pennsylvanian sequences, United States. In: F.T. Dulong and N.T. Edgar (Editors), AAPG Bulletin. American Association of Petroleum Geologists : Tulsa, OK, United States, pp. 1279-1280.

Cecil, C.B. and Edgar, N.T. (Editors), 2003. Special Publication - Society for Sedimentary GeologyClimate controls on stratigraphy. Special Publication - Society for Sedimentary Geology, 77. Society for Sedimentary Geology (SEPM) : Tulsa, OK, United States, United States.

Clifton, R.L., 1942. Invertebrate faunas from the Blaine and the Dog Creek formations of the Permian Leonard series. Journal of Paleontology, 16: 685-699.

Clifton, R.L., 1944. Paleoecology and environment inferred for some marginal middle Permian marine strata [Kansas, Oklahoma, Texas]. Bulletin of the American Association of Petroleum Geologists, 28: 1012-1031.

Cox, R. and Al-Shaieb, Z., 1980. Stratabound copper in Lower Permian red beds; North-central Oklahoma, Oklahoma Geology Notes. Oklahoma Geological Survey : Norman, OK, United States, pp. 191-192.

Dalrymple, R.W., Zaitlin, B.A. and Boyd, R., 1992. Estuarine facies models; conceptual basis and stratigraphic implications. Journal of Sedimentary Petrology, 62: 1130-1146.

Denison, R.E., Kirkland, D.W. and Evans, R., 1998. Using strontium isotopes to determine the age and origin of gypsum and anhydrite beds. Journal of Geology, 106: 1-17.

Dott, R.H., Jr. and Batten, R.L., 1971. Evolution of the Earth. McGraw-Hill Book Co., United States.

Dunham, R.J., 1962. Classification of carbonate rocks according to depositional texture. Memoir - American Association of Petroleum Geologists: 108-121.

Fay, R.O., 1962. Geology and mineral resources of Blaine County, Oklahoma; Part 1, Stratigraphy and general geology of Blaine County. Bulletin - Oklahoma Geological Survey, 89. Oklahoma Geological Survey : Norman, OK, United States, 1 pp.

Fay, R.O., 1964. Bulletin - Oklahoma Geological SurveyThe Blaine and related formations of northwestern Oklahoma and southern Kansas. Bulletin - Oklahoma Geological Survey. Oklahoma Geological Survey : Norman, OK, United States.

Fay, R.O. and Brockie, D.C., 2002. Special Publication - Oklahoma Geological SurveyMetallic-mineral resources of Oklahoma. Special Publication - Oklahoma Geological Survey. Oklahoma Geological Survey : Norman, OK, United States.

Fisher, J.A., Krapf, C.B.E., Lang, S.C., Nichols, G.J. and Payenberg, T.H.D., 2008. Sedimentology and architecture of the Douglas Creek terminal splay, Lake Eyre, central Australia. Sedimentology, 55: 1915-1930.

Fisher, W.L. and Rodda, P.U., 1969. Edwards Formation (Lower Cretaceous), Texas; dolomitization in a carbonate platform system. American Association of Petroleum Geologists Bulletin, 53: 55-72.

Fisk, H.N., 1959. Padre Island and the Laguna Madre Flats, coastal south Texas. In: R.J. Russell, chm. (Editor), Coastal Geography Conf. , pp. 103-151.

Galloway, W.E., 1975. Process framework for describing the morphologic and stratigraphic evolution of deltaic depositional systems. Houston Geol. Soc. : Houston, United States, 87-98 pp.

Glennie, K.W. and Evans, G., 1976. A reconnaissance of the Recent sediments of the Ranns of Kutch, India. Sedimentology, 23: 625-647.

Gould, C.N., 1924. A new classification of the Permian red beds of southwestern Oklahoma. Bulletin of the American Association of Petroleum Geologists, 8: 322-341.

Gould, C.N., 1926. The correlation of the Permian of Kansas, Oklahoma, and northern Texas. Bulletin of the American Association of Petroleum Geologists, 10: 144-153.

Green, D.A., 1936. Permian and Pennsylvanian sediments exposed in central and west-central Oklahoma. Bulletin of the American Association of Petroleum Geologists, 20: 1454-1475.

Green, D.A., 1937. Major Divisions of the Permian in Oklahoma and Southern Kansas. Bulletin of the American Association of Petroleum Geologist, 21(12): 1515-1533.

Gustavson, T.C., Presley, M.W., Handford, C.R., Finley, R.J., Dutton, S.P., Baumgardner, R.W., Jr., McGillis, K.A. and Simpkins, W.W., 1980. Geological Circular - Texas, University, Bureau of Economic GeologyGeology and geohydrology of the Palo Duro Basin, Texas Panhandle; a report on the progress of nuclear waste isolation feasibility studies (1979), Geological Circular - Texas, University, Bureau of Economic Geology. University of Texas at Austin, Bureau of Economic Geology : Austin, TX, United States.

Handford, C.R., 1981. Coastal sabkha and salt pan deposition of the lower Clear Fork Formation (Permian), Texas. Journal of Sedimentary Petrology, 51: 761-778.

Handford, C.R. and Fredericks, P.E., 1980. Geological Circular - Texas, University, Bureau of Economic GeologyFacies patterns and depositional history of a Permian sabkha complex; Red Cave Formation, Texas Panhandle. Geological Circular - Texas, University, Bureau of Economic Geology.

Hanshaw, B.B., Back, W. and Deike, R.G., 1971. A geochemical hypothesis for dolomitization by ground water. Economic Geology and the Bulletin of the Society of Economic Geologists, 66: 710-724.

Heine, R.R., 1975. Geochemistry and mineralogy of the Permian red beds and related copper deposits, Payne, Pawnee, and Noble Counties, Oklahoma, Oklahoma State University, Stillwater, OK, 70 pp.

Hills, J.M., 1942. Rhythm of Permian seas, a paleogeographic study. Bulletin of the American Association of Petroleum Geologists, 26: 217-255.

Holdoway, K.A., 1978. Bulletin - Kansas Geological SurveyDeposition of evaporites and red beds of the Nippewalla Group, Permian, western Kansas. Bulletin - Kansas Geological Survey. Kansas Geological Survey : Lawrence, KS, United States.

Holser, W.T. (Editor), 1966. Bromide geochemistry of salt rocks. North. Ohio Geol. Soc., Cleveland, Ohio, United States, 248-275 pp.

Holser, W.T., 1970. Bromide geochemistry of some non-marine salt deposits in the southern Great Basin. Special Paper - Mineralogical Society of America, 3: 307-319.

Hsu, K.J. and Schneider, J. (Editors), 1973. Progress Report on Dolomitization-Hydrology of Abu Dhabi Sabkhas, Arabian Gulf. The Persian Gulf. Springer-Verlag, New York, Federal Republic of Germany, 409-422 pp.

Johnson, K.S., 1967. Stratigraphy of the Permian Blaine Formation and associated strata in southwestern Oklahoma, University of Illinois at Urbana-Champaign, Urbana, IL, United States, 265 pp.

Johnson, K.S., 1972. Educational Publication - Oklahoma Geological SurveyGuidebook for Geologic Field Trips in Oklahoma, Book II; Northwest Oklahoma. Educational Publication - Oklahoma Geological Survey, 3. Oklahoma Geological Survey : Norman, OK, United States, United States.

Johnson, K.S., 1990. Standard outcrop section of the Blaine Formation and associated strata in southwestern Oklahoma. Oklahoma Geology Notes, 50: 144-168.

Johnson, K.S., 2003. Evaporite karst in the Permian Blaine Formation and associated strata of western Oklahoma, Circular - Oklahoma Geological Survey. University of Oklahoma : Norman, OK, United States, pp. 41-55.

Kammer, T.W., Brett, C.E., Boardman, D.R. and Mapes, R.H., 1986. Ecologic stability of the dysaerobic biofacies during the late Paleozoic. Lethaia, 19: 109-121.

Land, L.S., 1985. The origin of massive dolomite. Journal of Geological Education, 33: 112-125.

Lang, S.C., Payenberg, T.H.D., Reilly, M.R.W., Hicks, T., Benson, J.M. and Kassan, J., 2004. Modern analogues for dryland sandy fluvial-lacustrine deltas and terminal splay reservoirs, APPEA Journal. Australian Petroleum Production and Exploration Association : Canberra, Australia, pp. 329-356.

Long, D.T. and Gudramovics, R., 1983. Major-element geochemistry of brines from the Wind tidal flat area, Laguna Madre, Texas. Journal of Sedimentary Petrology, 53: 797-810.

Lucas, S.G., Heckert, A.B. and Hunt, A.P., 2001. Triassic stratigraphy, biostratigraphy and correlation in east-central New Mexico. Guidebook - New Mexico Geological Society, 52. New Mexico Geological Society : Socorro, NM, United States, United States, 85-102 pp.

Lucas, S.G., Rowland, J.M., Kues, B.S., Estep, J.W. and Wilde, G.L., 1999. Uppermost Pennsylvanian and Permian stratigraphy and biostratigraphy at Placitas, New Mexico, Guidebook - New Mexico Geological Society. New Mexico Geological Society : Socorro, NM, United States, pp. 281-292.

Mack, G.H., 2007. Sequence stratigraphy of the Lower Permian Abo Member in the Robledo and Dona Ana Mountains near Las Cruces, New Mexico. New Mexico Geology, 29. New Mexico Bureau of Geology and Mineral Resources : Socorro, NM, United States, United States, 3-12 pp.

Mack, G.H., Lawton, T.F. and Sherry, C.R., 1995. Fluvial and estuarine depositional environments of the Abo Formation (Early Permian), Caballo Mountains, south-central New Mexico. Bulletin - New Mexico Museum of Natural History and Science, 6. New Mexico Museum of Natural History and Science : Albuquerque, NM, United States, United States, 181-187 pp.

McKenzie, J.A., Hsu, K.J. and Schneider, J.F., 1980. Movement of subsurface waters under the sabkha, Abu Dhabi, UAE, and its relation to evaporative dolomite genesis. Special Publication - Society of Economic Paleontologists and Mineralogists: 11-30.

Miller, G.W. and Stanley, T.M., 2002. Geologic Map of the Blanchard 7.5' Quadrangle. Oklahoma Geological Survey.

Miller, J.A., 1975. Facies characteristics of Laguna Madre wind-tidal flats. Springer-Verlag : New York, N.Y., United States, United States, 67-73 pp.

Muhs, D.R. and Wolfe, S.A., 1999. Sand dunes of the Northern Great Plains of Canada and the United States. Bulletin - Geological Survey of Canada: 183-197.

Nichols, G.J. and Fisher, J.A., 2007. Processes, facies and architecture of fluvial distributary system deposits. Sedimentary Geology, 195: 75-90.

Olson, E.C., 1951. Fauna of upper Vale and Choza [Texas]; [Part] 1, A new family of the Parareptilia. Vertebrate paleontology, 10: 89-128.

Olson, E.C. and Mead, J.G., 1982. Bulletin of the Texas Memorial MuseumThe Vale Formation (Lower Permian); its vertebrates and paleoecology. Bulletin of the Texas Memorial Museum, 29.

Osborn, N.I., Eckenstein, E. and Fabian, R.S., 1998. Demonstration and evaluation of artificial recharge to the Blaine Aquifer in southwestern Oklahoma. Oklahoma Geology Notes, 58. Oklahoma Geological Survey : Norman, OK, United States, United States, 184-207 pp.

Paxton, S.T., Gromadzki, G.A., Kenney, K. and Abbott, B.N., 2004. A geological framework for the occurrence and distribution of naturally-occurring arsenic in the Permian (Leonardian) Garber-Wellington Aquifer, central Oklahoma, Abstracts with Programs - Geological Society of America. Geological Society of America (GSA) : Boulder, CO, United States, pp. 564-564.

Pendery, E.C., III, 1963. Stratigraphy of Blaine Formation (Permian), north-central Texas. Bulletin of the American Association of Petroleum Geologists, 47: 1828-1839.

Peyser, C.E. and Poulsen, C.J., 2008. Controls on Permo-Carboniferous precipitation over tropical Pangaea; a GCM sensitivity study. Palaeogeography, Palaeoclimatology, Palaeoecology, 268: 181-192.

Presley, M.W., 1981. Permeable sheet sandstones of the Glorieta Formation intertongue with salt-bearing rocks in the northwestern Texas Panhandle, Geological Circular - Texas, University, Bureau of Economic Geology. University of Texas at Austin, Bureau of Economic Geology : Austin, TX, United States, pp. 10-18.

Presley, M.W., 1987. Evolution of Permian evaporite basin in Texas Panhandle. AAPG Bulletin, 71: 167-190.

Retallack, G.J., 1990. Soils of the past; an introduction to paleopedology. Unwin Hyman : Boston, MA, United States, United States.

Sawyer, R.W., 1924. Areal geology of a part of southwestern Oklahoma (with discussion by F. C. Greene and others). Bulletin of the American Association of Petroleum Geologists, 8: 312-321.

Sibley, D.F. and Gregg, J.M., 1987. Classification of dolomite rock textures. Journal of Sedimentary Petrology, 57: 967-975.

Soreghan, G.S., Soreghan, M.J. and Hamilton, M.A., 2008a. Origin and significance of loess in late Paleozoic western Pangaea; a record of tropical cold? Palaeogeography, Palaeoclimatology, Palaeoecology, 268: 234-259.

Soreghan, M.J. and Soreghan, G.S., 2007. Whole-rock geochemistry of upper Paleozoic loessite, western Pangaea; implications for paleo-atmospheric circulation. Earth and Planetary Science Letters, 255: 117-132.

Soreghan, M.J., Soreghan, G.S. and Hamilton, M.A., 2008b. Glacial-interglacial shifts in atmospheric circulation of western tropical Pangaea. Palaeogeography, Palaeoclimatology, Palaeoecology, 268: 260-272.

Speer, S.W., 1983. Abo Formation, north-central Sacramento Mountains; an onlapping fluvial clastic wedge. N.M. Bur. Mines and Miner. Resour. : Socorro, NM, United States, United States, 54-72 pp.

Suneson, N.H. and Stanley, T.M., 2001. Geologic Map of the Oklahoma City SW 7.5' Quadrangle. Oklahoma Geological Survey.

Tabor, N.J. and Montanez, I., 2005. Oxygen and hydrogen isotope compositions of Permian pedogenic phyllosilicates; development of modern surface domain arrays and implications for paleotemperature reconstructions. Palaeogeography, Palaeoclimatology, Palaeoecology, 223: 127-146.

Tabor, N.J. and Montañez, I.P.M., 2004. Morphology and distribution of fossil soils in the Permo-Pennsylvanian Wichita and Bowie Groups, north-central Texas, USA: implications for western equatorial Pangean palaeoclimate during icehouse&;greenhouse transition. Sedimentology, 51(4): 851-884.

Talbot, M.R., Holm, K. and Williams, M.A.J., 1994. Sedimentation in low-gradient desert margin systems; a comparison of the Late Triassic of Northwest Somerset (England) and the late Quaternary of east-central Australia. Special Paper - Geological Society of America, 289: 97-117.

Thompson, R.W., 1968. Memoir - Geological Society of AmericaTidal flat sedimentation on the Colorado River delta, northwestern Gulf of California. Memoir - Geological Society of America, 107. Geological Society of America (GSA) : Boulder, CO, United States, United States.

Thompson, R.W., 1975. Tidal-flat sediments of the Colorado River delta, northwestern Gulf of California. Springer-Verlag : New York, N.Y., United States, United States, 57-65 pp.

Tomlinson, C.W., 1916. The origin of the red beds; a study of the conditions of origin of the Permo-Carboniferous and Triassic red beds of the western United States. Journal of Geology: 153-179.

Tooth, S., 1999. Floodouts in central Australia. Geomorphology Publication - International Association of Geomorphologists, 7: 219-247.

Tooth, S., 2005. Splay formation along the lower reaches of ephemeral rivers on the Northern Plains of arid central Australia. Journal of Sedimentary Research, 75: 636-649.

Tucker, M.E., Wright, V.P. and Dickson, J.A.D., 1990. Carbonate sedimentology. Blackwell Sci. Publ. : Oxford, United Kingdom, United Kingdom.

Yang, S.-R.V., 1985. Petrological and geochemical approaches to the origin of the San Angelo-Flowerpot red beds (Permian) and their associated stratiform copper mineralizations in north central Texas and southwestern Oklahoma, United States.

APPENDIX

Appendix #1-XRD methods taken directly from Steve Chipera

X-ray Diffraction Analyses:

To prepare the samples for X-ray powder diffraction analysis (XRD), a small portion of each sample (~1.6 g) was mixed with 1.0-μm corundum (Al_2O_3) internal standard in the ratio 80% sample to 20% corundum by weight. Each sample was then ground under acetone in an McCrone Micronizing mill (fitted with an agate grinding set) for a time of approximately 10 minutes. This produced a sample with an average particle size of less than 5 μm and ensured thorough mixing of sample and internal standard. The fine particle size is necessary to ensure adequate particle statistics and to reduce primary extinction and other sample-related effects (Bish and Reynolds 1989; Klug and Alexander 1974).

All diffraction patterns were collected on a Bruker D4 X-ray powder diffractometer using CuKα radiation and a Bruker VANTEC position sensitive detector, from 2–70°2θ, using ~0.02° steps, and counting for at least 2s/step. Samples were mounted in a circular back-pack-mount machined out of aluminum and anodized.

Mineral abundances were determined using FULLPAT, a quantitative X-ray powder diffraction (QXRD) program and method developed in the Earth and Environmental Sciences Division at Los Alamos National Laboratory (Chipera and Bish, 2002). FULLPAT matches entire patterns including the background, and utilizes a least-squares refinement to optimize the fitting of the library standards to the observed pattern. The advantage of FULLPAT over the other QXRD methods is that amorphous components are now explicitly analyzed by fitting the entire background. FULLPAT no longer requires that the amorphous abundance be constrained as the difference from 100% (i.e. amorphous abundance = 100% - sum of phases abundances for the crystalline phases). Like the traditional RIR method but unlike the other full-pattern methods, all library standards and samples are mixed with corundum as an internal standard to compensate for matrix effects so that an unconstrained analysis can be made. Fitting of entire patterns alleviates many of the problems encountered with the traditional RIR methods of quantitative analyses (see Bish and Chipera, 1988; 1995 for a more complete discussion). FULLPAT has an advantage over the Rietveld method (Bish and Howard, 1988) in that the Rietveld method requires that a crystal structure be known for all the phases and that the phases all exhibit 3-dimensional order – which is not the case for clay minerals.

Clay Mineral Analyses:

Clay mineral analyses are conducted by disaggregating an aliquot of sample suspended in de-ionized water with an ultrasonic probe for about 10 minutes. Sample is then centrifuged to sediment out the larger than 1.0μm fraction. The <1.0μm fraction which is still in suspension is then vacuum filtered onto silver-membrane filters. Samples are immersed overnight into an ethylene-glycol atmosphere inside of an oven held at 80ºC and then X-rayed. The large organic molecules go into the clay interlayers to determine the amount of expandable layers in the I/S. Expansion is approximated by comparing the patterns to calculated patterns generated by the NEWMOD computer program written by Robert Reynolds, Jr. Details of these analyses can be found in Moore and Reynolds

(1989). Illite is composed of 100% collapsed layers. Pure smectite has 100% expandable layers (i.e., swells with the introduction of water). Mixed-layer illite/smectite (I/S) is used when the clay has both expandable and collapsed layers. In the case of your samples, the I/S comprises about 10-15% of the rock and is itself composed of about 20% expandable layers. To get a qualitative sense on rock behavior due to the swelling of clays, we can multiply the percentage of the I/S times the amount of expandable layers to put it in a relative % of expandable layers in the rock basis.

VITA

Tyler Treece

Candidate for the Degree of

Master of Science

Thesis: FACIES ARCHITECTURE OF AN ARID COASTLINE WITHIN THE PERMIAN ROCKS OF WESTERN OKLAHOMA

Major Field: Geology

Biographical:

Personal Data: Born in Fort Smith, Arkansas on March 29, 1985, the son of V. Scott and Pamm S. Treece.

Education: Graduated from Alma High School, Alma, Arkansas in May 2003; received a Bachelor of Science degree in Professional Geology from Arkansas Tech University, Russellville, Arkansas in May 2007. Completed the requirements for the Master of Science in Geology at Oklahoma State university, Stillwater, Oklahoma in July, 2009.

Experience: Employed by Oklahoma State University, Boone Pickens School of Geology as a graduate teaching and research assistant, 2007-2009; employed as a geological Intern at Chesapeake Energy Corporation, Oklahoma City, OK, summer 2008; employed as a geological intern at Valley Exploration Inc., Fort Smith, Arkansas, 2006-2007; employed as a laboratory teaching assistant at Arkansas Tech University, 2005-2007.

Professional Memberships: American Association of Petroleum Geologist; Geological Society of America; SEPM; Oklahoma City Geological Society

.

Name: Tyler Monk Treece   Date of Degree: July, 2009

Institution: Oklahoma State University   Location: Stillwater, Oklahoma

Title of Study: FACIES ARCHITECTURE OF AN ARID COASTLINE WITHIN THE PERMIAN ROCKS OF WESTERN OKLAHOMA

Pages in Study: 63   Candidate for the Degree of Master of Science

Major Field: Geology

Scope and Method of Study: Deposits of the El Reno Group (Permian) of central Oklahoma are represented by the Flowerpot Shale, Blaine Formation, Dog Creek Shale, and Duncan Formation. These deposits were studied through geological mapping, measuring section, and analyzing thin sections and XRD data.

Findings and Conclusions: The Duncan Formation represents proximal deposits that grade into distal deposits of the Flowerpot Shale, Blaine Formation, and Dog Creek Shale. The classic flooding sequence for the Blaine Formation is represented by: 1) inundation with lacustrine or possibly marine water resulting in the deposition of carbonate (dolomites), 2) evaporation of water to the point of gypsum deposition, and 3) mudstone deposition during periods of no water. Six facies were identified within the Duncan Formation: 1) mudstone conglomerate; 2) clay layers; 3) ripple-cross laminated very fine-grained sandstone; 4) fine to medium sandstone with large-scale low-angle trough cross beds; 5) clean fine-grained sandstone with high-angle trough cross beds and root casts; and 6) shale-mudstone. Analogs can be drawn between the El Reno Group and facies described in the Douglas Creek terminal splay of central Australia and other sabkha systems. This comparison supports an interpretation that the Duncan Formation was deposited on the edge of an intracontinental basin as a terminal splay complex and the other units of the El Reno Group represent deposits from a continental sabkha-like system. An arid-land depositional environment may provide a better analogue when trying to interpret the Red Beds of the North American mid-continent than traditional depositional models.

ADVISER'S APPROVAL: Dr. Alexander R. Simms

Geological Map Northern Canadian County, Oklahoma, USA

Explanation

Qds
Dune Sand
Wind-blown sand; thickness ranges from thin veneer to 8 meters

Qt
Terrace Deposits
Stream-laid deposits of sand, silt, clay, gravel, and volcanic ash; thickness ranges from 0 to 15 meters

Qal
Alluvium
Stream-laid deposits of sand, silt, clay, gravel; thickness ranges from 0 to 30 meters

UNCONFORMITY

Pdc
Dog Creek Shale
Mostly red-brown silty shale and some fine-grained sandstone. Contains one or two layers of thin dolomite (or gypsum) in lower part.

Pb
Blaine Formation
Mostly red-brown shale interbedded with thin dolomites and associated gypsums; grades into the Duncan Formation toward the Southwest.

Pd
Duncan Formation
Variegated mudstone conglomerate, red-brown to orange-brown silty shale and siltstone, and fine to medium-grained sandstone; grades into Flowerpot Shale, Blaine Formation, and Dog Creek Shale.

Pf
Flower Pot
Mostly red-brown silty clay shale with stringers of gypsum (satin spar); grades inton the Duncan Formation toward the Southwest.